Comparing advanced control strategies to eliminate stick-slip oscillations in drillstrings

Jean Auriol, Islam Boussaada, Roman J. Shor, Hugues Mounier, Silviu-Iulian Niculescu

IEEE Access
Multidisciplinary | Rapid Review | Open Access Journal

Digital Object Identifier

Comparing advanced control strategies to eliminate stick-slip oscillations in drillstrings

JEAN AURIOL[1] (IEEE MEMBER), ISLAM BOUSSAADA[1,2,3] (IEEE MEMBER), ROMAN J. SHOR[4], HUGUES MOUNIER[1], SILVIU-IULIAN NICULESCU[1,2] (IEEE FELLOW),

[1]Université Paris-Saclay, CentraleSupélec, CNRS, Laboratoire des signaux et systèmes, Gif-sur-Yvette, France.
[2]Inria Saclay, DISCO Team, France
[3]IPSA, France
[4]Department of Chemical and Petroleum Engineering, University of Calgary, Calgary, Alberta, Canada

Corresponding author: Jean Auriol (e-mail: jean.auriol@centralesupelec.fr).

ABSTRACT

In this paper, we present three methods to achieve reliable drillbit angular velocity control for deep drilling operations. We consider a multi-sectional drilling system with the bit off-bottom, which represents the system at the start-up of a drilling operation, e.g., after a connection. The three control procedures are all based on a distributed model for the drilling system. The proposed model has been field validated and considers Coulomb friction between the drillstring and the borehole. The first algorithm we propose combines the industry standard ZTorque controller with a feedforward component. The second procedure is based on a multiplicity-induced-dominancy (MID) design that corresponds to a pole-placement for the downhole state. Finally, the last class of controllers relies on a recursive interconnected dynamics framework. All the controllers are combined with a disturbance rejection procedure whose design is based on a switching-mode approach. These three algorithms are illustrated in simulations with field scenarios on several test-cases. Their complexities, effectiveness and limitations regarding industrial implementation criteria are discussed.

INDEX TERMS drillstring vibrations, stick-slip, downhole boundary, bit off-bottom, distributed systems, ODE-PDE-ODE system, differential flatness, delay equations, multiplicity-induced-dominancy (MID), performance analysis

I. INTRODUCTION

EXTRACTION of resources in the earth's subsurface - oil, gas, minerals, and thermal energy - necessitates drilling long slender boreholes from the surface to the subsurface target. The diameters of the wells required to extract these resources range from 10 to 50 cm, and lengths can frequently exceed 10,000 m, leading to mechanical systems with extreme aspect ratios. These drillstrings consist of sections of steel drill pipe and stiffer drill collars. These systems are the source of complex dynamic behaviors as many dynamic phenomena are involved such as vibrations, bending and twisting quasi-static motion, and bit-rock interactions [1], [2]. In particular, the drillstring interaction with the borehole gives rise to a wide variety of undesired oscillations [3]–[5] which can be classified depending on the direction they appear. Among these oscillations, torsional vibrations can appear due to downhole conditions (such as significant drag, tight annular clearances or formation characteristics [6] for instance) or due to side forces induced by Coulomb friction terms [7]. These oscillations are known as *stick-slip* and are considered to be the most destructive as they may cause fatigue of the equipment, a deterioration of the performance of the process, or a premature failing of the bit [8]. This may result in catastrophic damages and at least wear to expensive components of the drillstring [9]. These oscillations are characterized by a series of *stick* (a cessation of bit rotation) and *slip* (a sudden release of energy) cycles [10], [11].

As a clear understanding of drillstring dynamics appears to be crucial to control these vibrations and consequently improve the performance of drilling systems (Rate Of Penetration) or prevent any eventual damage and reduce safety risks, a wide range of models have been proposed in the literature to explain stick-slip oscillations. In the simplest mod-

els, stick-slip oscillations are induced from a non-linearity of the frictional force at the bit. More precisely, the bit-rock interaction takes the form of a discontinuous frictional force at the bit. A simplified formulation of drillstring dynamics can be modeled as a lumped mass, representing the bottom hole assembly (BHA) inertia combined with a torsional spring, representing the drillstring stiffness [12], [13]. More complex models have been introduced in [6], [14]. However, it has been observed that stick-slip oscillations can occur off-bottom and do not require a velocity weakening in the bit–rock interaction. The aforementioned simple models do not properly encompass this well-known phenomenon from the field. It is hypothesized to be caused by a negative difference between static and kinetic *along-string* Coulomb-type friction [15]–[17]. This cause is distinct from the regenerative effect in the bit–rock interaction which is already known to generate stick-slip oscillations, particularly in vertical or near vertical wells [18], [19]. This is particularly important in modern wellbores, which are rarely straight and must follow pre-planned well plans, ranging from simpler horizontal or deviated wells to complex three-dimensional paths, thus increasing the effect of torque and drag. In this context, distributed models appear to be more relevant to characterize stick-slip oscillation. In the model proposed in [7], the drillstring dynamics are modeled as a set of hyperbolic Partial Differential Equations (PDEs), namely wave equations, coupled with Ordinary Differential Equations (ODEs) through their boundaries. Such a model encompasses Coulomb friction-induced side forces using an inclusion term. We will use this class of models in the present paper.

During the drilling process, the operator usually seeks to control the downhole behavior of the drillstring (e.g., reach a given angular velocity or a given orientation.) and optimize the Rate Of Penetration (ROP) while avoiding undesired oscillations. It is usually possible to impose (using the top drive) the weight on the drillstring and the torque at the surface. Through the last decades, a significant research effort has been conducted to design various types of stick-slip mitigation controllers in order to fulfill these control objectives [11], [20]. In our opinion, this explains why a large variety of stick-slip mitigation controllers can be found in the literature: Proportional-Integral-Derivative (PID) controllers [21], impedance matching controllers [22], sliding mode controllers [23], and others [24], [25]. Most of the controllers applied in industrial applications correspond to high-gains PI control laws, following the SoftSpeed and SoftTorque approaches. These approaches are easy to implement and to analyze since the gains are tuned to obtain a certain reduction in the proximal reflection coefficient over a limited frequency range [26]. However, they may present several fundamental limitations as possible poor inherent robustness margins [27] (which can be overcome using impedance matching controllers such as ZTorque [22]) or the generation of significant oscillations when changing the set-points. Moreover, the Coulomb side-forces effect is not always well compensated by such PI control laws. Consequently, a flatness-based approach has been developed in [28] to cancel the impact of the Stribeck-like effect of the torque acting on the BHA as rotation is initiated. The control law then combines three terms: a feed-forward term to compensate the effect of the Coulomb friction terms, a trajectory term, and a stabilization term (that corresponds to a ZTorque PI controller), thus conforming to the canonical 3-DOF controller design for tracking and disturbance rejection. Such an add-on requires a minimal implementation effort for practitioners. However, it has only been designed for a uni-sectional pipe and may not handle the case of multi-sectional drillstring where the different segments of pipe that compose the drillstring may have different physical properties (as weight, diameter, or inertia). Indeed, the change of the characteristic line impedance may cause reflections in the traveling waves and deteriorate the performance of the closed-loop system. In addition, although simple to implement, the stabilizing part of the controller still corresponds to a PI control law (SoftTorque or ZTorque). The incentive to do so is to reduce the computational effort and preserve a simple controller architecture. However, explicitly taking into account the delays and high-frequency content in the model should lead to overall increased performance with respect to a given set of specifications. Indeed, the torsional dynamics of a drilling system corresponds to an interconnected system composed of ODEs coupled with wave equations. Several controllers have already been developed for such systems in the literature (at least in a theoretical framework). For instance, the *multiplicity induced-dominancy* (MID) property was outlined in [29], [30] for retarded time-delay systems and extended to neutral delay differential equations of orders 1 and 2 [31]–[33] (a mathematical class of systems to which the dynamics considered in this paper belong). The MID property was established in a general framework in [34] for generic retarded delay differential equations. It relies on existing links between quasipolynomials with a real root of maximal multiplicity and Kummer's confluent hypergeometric function in terms of the location of the characteristic roots. Such an approach opens interesting perspectives in control design, such as the systematic tuning of the gains of the well-known PID controller [31]. It consists of two steps: the first step, which is a quasipolynomial interpolation, corresponds to forcing a spectral value to have a prescribed admissible multiplicity; the second step consists in establishing the conditions in the parameters guaranteeing such a multiple spectral value to be dominant (i.e., the remaining spectral values of the closed-loop system are located to the left of the assigned poles [35], [36]). More recently, another control strategy has been proposed in [37] using a recursive dynamics interconnection framework. Roughly speaking, the control law is recursively obtained by considering stabilizing virtual inputs for each subsystem and by ensuring the outputs of each subsystem converge to these desired virtual inputs. This recursive framework can also be used to estimate the boundary states. Such control laws could be potential competitors with

the SoftTorque/ZTorque control laws.

In this paper, we present the derivation of and compare three different control strategies to achieve angular velocity control in the case of a multi-sectional drillstring with the bit off-bottom. The three control approaches correspond to the extension of the ZTorque feedforward control law proposed in [28], to a MID-based controller (that extends the control law proposed in [33]) and to a recursive dynamics inter-connection framework [37]–[39]. All the controllers are based on the infinite-dimensional model proposed in [28]. These controllers are coupled with a disturbance compensation strategy that compensates for the effects of the Coulomb friction terms. This compensation of the disturbance relies on a switching-mode procedure. We first guarantee the release of the BHA from the stick phase by setting the control input to an arbitrarily large value. The disturbance term then becomes constant and can be easily removed. The three control procedures present an increasing order of complexity. They will be compared with respect to performance indices adjusted from classical industrial implementation specifications which include ease of implementation (both computationally and difficulty of integration in industrial motor controllers), performance and robustness to latency and delay. Such a comparison is crucial to improve the overall performance of the drilling operations. Some of these algorithms may require an estimation of the distributed states. Although an adaptive soft sensor has been proposed in [40] for the case of a single-sectional drillstring, we present here a new type of estimator, which is based on our recursive dynamics framework.

More precisely, the contribution of the paper is three-fold. First, we extend the feed-forward control strategy proposed in [28] to the case of a multi-sectional drillstring. Then, we propose two new alternative control strategies and a simple real-time estimation procedure of the state. Finally, we compare the different algorithms for several industrial implementation criteria. This comparison will be made against a high-fidelity model derived from [28].

The paper is organized as follows. In Section II, we present the torsional model we utilize in this paper to describe the torsional motion of a multi-sectional drilling system with the bit off-bottom. The model is adopted from [7] where it was validated against field data. We also present the control objectives and specifications before introducing the different control strategies. The ZTorque feed-forward controller is presented in Section III. The second class of controllers corresponds to neutral-type (MID) controllers and is derived in Section IV. Finally, the last class of controllers we consider relies on a recursive interconnected dynamics framework and is described in Section V. A disturbance rejection procedure is introduced in Section VI. We present in Section VII a state-observer that can be used to design output-feedback controllers. In Section VIII, we compare the different controllers against field scenarios. We give some remarks about implementation requirements in Section IX. Some concluding remarks are given in Section X.

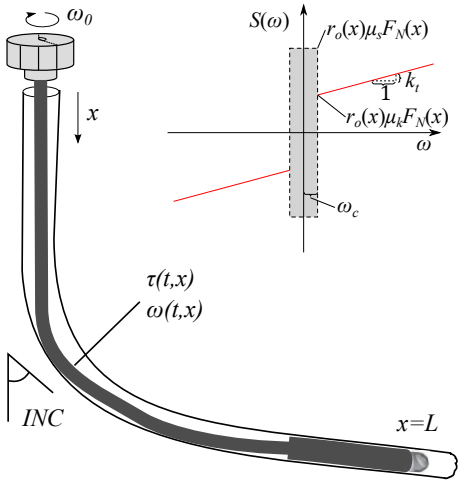

FIGURE 1: Schematic showing a two segment drillstring of length L lying in a deviated borehole. Inset: Schematic illustrating the friction source term $S(\omega, x)$. The shaded region represents the angular velocities for which a constant value of static torque is assumed and the red curve indicates the dynamic torque as a function of angular velocity (figure from [7]).

II. TORSIONAL VIBRATIONS MODEL

This section summarizes a hyperbolic partial differential equations model with distributed friction terms to describe the torsional motion of a drilling device. A full derivation of the high-fidelity model is given in [7] where it was validated against field data. Its computational simplicity allows it to be used in control and estimation applications. Since the objective of the proposed contribution is to compare the performance of different control strategies, it is reasonable to perform this comparison in the most amenable case. The main assumptions are as follows:

- Torsional motion is the dominant dynamic.
- Static and dynamic friction is modeled as a jump, i.e., the Stribeck curve is assumed negligible.
- The effect of along-string cuttings distribution is assumed constant and homogeneous.
- The effect of the pressure differential, inside and outside the drillstring, on the bending moment is not represented and is assumed to be negligible.
- As we are investigating the performance of each control during start-up, the bit is off-bottom which means there is no bit-rock interaction.

These assumptions are consistent with the ones given in [7] and are reasonable when considering that the bit is off-bottom.

A. DISTRIBUTED TORSIONAL DYNAMICS

We model the dynamics of a directional drilling system of length L (Figure 1). In this model, x denotes the curvilinear abscissa, $x = 0$ is the position of the top-drive, while $x = L$ is the position of the drill bit. The torsional motion of the

drillstring is assumed to be the dominating dynamic behavior, which is particularly true at the start of rotation after a connection. The torsional dynamics is represented using the popular model (see [7], [41]) of a distributed wave model where discontinuities in impedance can be included to model different sections of the drillstring, such as a pipe and a collar section. We refer to [7] for the full model derivation.

A schematic representation of the drillstring is given in Fig. 1. Let us denote $\Phi(t,x)$ the rotary angle of the drillstring. It is a function of (t,x) evolving in $\{(t,x) \mid 0 < t < T,\ x \in [0,L]\}$ (where T is positive time). We denote the angular velocity and torque as $\omega(t,x), \tau(t,x)$, respectively, with $(t,x) \in [0,\infty) \times [0,L]$ (L being the length of the drillstring). The angular torque associated to Φ can be found from the strain, given as the local relative compression:

$$\tau(t,x) = JG\frac{(\Phi(t,x) - \Phi(t,x+dx))}{dx}, \tag{1}$$

J being the polar moment of inertia, G the shear modulus and $dx \to 0$ the infinitesimal position increment. The angular velocity satisfies

$$\omega(t,x) = \frac{\partial \Phi(t,x)}{\partial t}.$$

The diameter to length ratio of a drillstring, typically less than 10^{-4}, implies that the drillstring can be modeled using an Euler–Bernoulli beam model. More precisely, we can derive the dynamics of interest by assuming elastic deformations and using equations of continuity and state. The torsional motion satisfies the following wave partial differential equations (that can be found in [7])

$$\frac{\partial \tau(t,x)}{\partial t} + JG\frac{\partial \omega(t,x)}{\partial x} = 0, \tag{2}$$

$$J\rho\frac{\partial \omega(t,x)}{\partial t} + \frac{\partial \tau(t,x)}{\partial x} = -k_t\rho J\omega(t,x) - \mathcal{F}(t,x), \tag{3}$$

where ρ is the drillstring density, and where the damping constant k_t represents the viscous shear stresses. We will denote $c_t = \sqrt{\frac{G}{\rho}}$ as the torsional propagation velocity. The function $\mathcal{F}(t,x)$ that appears in equation (3) is a differential inclusion that represents the Coulomb friction between the drillstring and the borehole, also known as the side force. This side force is modeled using the following inclusion [7]

$$\begin{cases} \mathcal{F}(t,x) = r_o(x)\mu_k F_N(x), & \omega(t) > \omega_c, \\ \mathcal{F}(t,x) \in \pm r_o(x)\mu_s F_N(x), & |\omega(t)| \le \omega_c, \\ \mathcal{F}(t,x) = -r_o(x)\mu_k F_N(x), & \omega(t) < -\omega_c, \end{cases} \tag{4}$$

where μ_s is the static friction coefficient (i.e. the friction between two or more solid objects that are not moving relative to each other) and μ_k is the kinetic friction coefficient (also known as dynamic friction or sliding friction, which occurs when two objects are moving relative to each other and rub together), ω_c is the threshold on the angular velocity where the Coulomb friction transits from static to dynamic, $r_o(x)$ is the outer drillstring radius. The function F_N is the normal force acting between the drillstring and the borehole wall. The function $\mathcal{F}(t,x) \in \pm r_o(x)\mu_s F_N(x)$ (that needs to be computed when $|\omega(t)| < \omega_c$) denotes the inclusion where

$$\begin{aligned} \mathcal{F}(t,x) &= -\frac{\partial \tau(t,x)}{\partial x} - k_t\rho J\omega(t,x) \\ &\in [-r_o(x)\mu_s F_N(x), r_o(x)\mu_s F_N(x)], \end{aligned} \tag{5}$$

and takes the boundary values $\pm\mu_s F_N(x)$ if this relation does not hold.

Using the torque model of [42] it is possible to derive the normal force profile $F_N(x)$ (see [7] for details). We consider in this work that the different constant physical parameters are perfectly known. In particular, the friction factors and the velocity threshold are known, which can appear as a restrictive condition. However, an adaptive soft sensor has been proposed in [40] to estimate these parameters. This soft sensor only requires sampled top-drive angular velocity measurements that are available during typical drilling operations. The control strategies we present in this paper can then be combined with such an observer.

B. DISCONTINUITIES OF A MULTIPLE SECTIONED DRILLSTRING

The drillstring is usually made up of different segments of pipes. For instance, the lower part of the drillstring is made up of drill collars that may have a great impact on the global dynamics due to their high inertia [43]. In particular, these pipes may have different lengths, density, inertia or Young's modulus. This change of the characteristic line impedance may cause reflections in the traveling waves. Let us assume we have N different sections ($N \in \mathbb{N}$), and let us denote x_i the spatial coordinate of the junction point between the $(i)^{\text{th}}$-section and the $(i+1)^{\text{th}}$-section. Let us denote $x_0 = 0$, $x_N = L$ and $(\tau^i(t,x),\ \omega^i(t,x))$ the torque and angular velocity along the i^{th} section of the drillstring. The corresponding physical parameters will also be expressed using the superscript ^{i} (for instance ρ^i will be the density of the i^{th} section). The boundary conditions at the transition are given by the following continuity constraints

$$\tau^i(t,x_i) = \tau^{i+1}(t,x_i), \quad \omega^i(t,x_i) = \omega^{i+1}(t,x_i). \tag{6}$$

When there is no ambiguity, this superscript will be omitted to ease the notations.

C. TOP-DRIVE BOUNDARY CONDITIONS

The drillstring is connected at the top to the *top-drive* suspended over the drill floor by the *traveling block*. This top-drive is actuated by a motor torque $u_T = \tau_m$. This yields

$$I_{TD}\frac{\partial \omega(t,x)}{\partial t}|_{x=0} = u_T(t) - \tau(t,0), \tag{7}$$

In what follows, we denote $\omega_{TD} = \omega(t,0)$ and $\tau_{TD} = \tau(t,0)$ as the angular velocity and torque at the top of the drillstring. Similarly, we will denote $\omega_{DH} = \omega(t,L)$ and $\tau_{DH} = \tau(t,L)$ as the angular velocity and torque at the bottom of the drillstring.

D. DOWNHOLE BOUNDARY CONDITION: LUMPED BHA

Since the bit is off-bottom, the torque at the bottom of the drillstring is equal to zero: $\tau_{DH}(t) = 0$. However, as Bottom Hole Assemblies (BHAs) often consist of a variety of different drilling or sensing tools, stabilizers and drill collars, it is desirable to approximate the BHA section as a single lumped inertial element to simplify the analysis (series of rigid bodies connected by springs). This approximation is justified because the length of the BHA ($\approx$ 200m) is much smaller than the one of the drillstring ($\approx$ 2000m). Moreover, much of the torque acting on the drillstring will come from stabilizers located in, or close to, the BHA. Thus, the source-terms acting on (3) can be lumped into an ODE coupled with the drillstring [28], [44], [45]. Another reason to consider an ODE at the BHA is that this kind of structure naturally appears when dealing with bit-rock interaction. The inertia of the lumped BHA is given by

$$I_{BHA} = \rho_{BHA} L_{BHA} J_{BHA}, \tag{8}$$

where ρ_{BHA} and J_{BHA} are the average density and polar moment of inertia of the BHA, while L_{BHA} is its length. The downhole boundary condition at $x = L$ can then be obtained from a torque balance on the lumped BHA. This yields

$$\frac{d}{dt}\omega_{DH}(t) = \frac{1}{I_{BHA}}(\tau_{DH}(t) - d(t)), \tag{9}$$

where $\omega_{DH}(t) = \omega(t, L_p)$ and $\tau_{DH}(t) = \tau(t, L_p)$ (L_p being the length of the pipe before the lumped section), where $d(t)$ accounts for the now lumped effect of the distributed source term, i.e.:

$$d(t) = \int_0^L (\mathcal{F}(t,x) - k_t \rho \omega(t,x))dx. \tag{10}$$

The function $d(t)$ can then be seen as a disturbance acting on the downhole boundary condition. An evaluation of the error introduced by the lumped approximation has been derived in [28]. Using this lumped approximation of the BHA, we obtain what is sometimes referred as the semi-lumped approximation. This approximation for the dynamics of the BHA simplifies the simulation of the system (as the BHA could be composed of a large number of pipes) and the mathematical analysis as the disturbance terms are now lumped at the boundary. It results in an ODE-PDE-ODE configuration, the first ODE corresponds to the top-drive dynamics, the second ODE being the lumped BHA. Note that such an ODE-PDE-ODE configuration naturally appears when considering bit-rock interaction [18], [46]. The system can now be rewritten as

$$\frac{\partial \tau^i(t,x)}{\partial t} + J^i G^i \frac{\partial \omega^i(t,x)}{\partial x} = 0 \tag{11}$$

$$J^i \rho^i \frac{\partial \omega^i(t,x)}{\partial t} + \frac{\partial \tau^i(t,x)}{\partial x} = 0 \tag{12}$$

with the boundary conditions

$$I_{TD}\dot{\omega}_{TD}(t) = u_T(t) - \tau_{TD}(t), \tag{13}$$

$$I_{BHA}\dot{\omega}_{DH}(t) = \tau_{DH}(t) - d(t), \tag{14}$$

and the continuity conditions

$$\tau^i(t,x_i) = \tau^{i+1}(t,x_i), \quad \omega^i(t,x_i) = \omega^{i+1}(t,x_i). \tag{15}$$

Remark 1: In the proposed lumped model, the effect of the disturbance term induced by the Coulomb friction only acts on the downhole boundary condition (ODE). For a multi-sectional drilling device, it may appear more accurate to consider several disturbance terms $d_i(t)$ that account for the lumped effect of the distributed source term on each subsection. Such terms would appear on the continuity conditions (15). Although these terms make the analysis more complex, the procedures we propose in this paper can easily be adjusted to encompass them.

E. RIEMANN INVARIANTS

The Riemann invariants of a hyperbolic PDE are the states that correspond to a transformation of the system for which the transport matrix has been diagonalized, i.e. the system can be written as a series of transport equations only coupled through the source terms [47]. For each subsection, we denote the Riemann invariants as $\alpha^i(t,x)$ and $\beta^i(t,x)$ with $(t,x) \in [0,\infty) \times [0,L]$. They are defined by

$$\alpha^i = \omega^i + \frac{c_t^i}{J^i G^i}\tau^i, \quad \beta^i = \omega^i - \frac{c_t^i}{J^i G^i}\tau^i, \tag{16}$$

where we recall that the torsional propagation velocity is defined by $c_t^i = \sqrt{\frac{\rho^i}{J^i}}$. Consequently, on each subsection, the Riemann invariants verify

$$\frac{\partial \alpha^i(t,x)}{\partial t} + c_t^i \frac{\partial \alpha^i(t,x)}{\partial x} = 0, \tag{17}$$

$$\frac{\partial \beta^i(t,x)}{\partial t} - c_t^i \frac{\partial \beta^i(t,x)}{\partial x} = 0. \tag{18}$$

In the Riemann coordinates, the boundary conditions at the junctions (6) rewrite for $1 < i < N$

$$\alpha^{i+1}(t,x_i) = a_1^i \alpha^i(t,x_i) + a_2^i \beta^{i+1}(t,x_i), \tag{19}$$

$$\beta^i(t,x_i) = a_3^i \alpha^i(t,x_i) + a_4^i \beta^{i+1}(t,x_i), \tag{20}$$

where

$$a_1^i = \frac{2}{1+Z^i},\ a_2^i = \frac{Z^i - 1}{1+Z^i},\ a_3^i = \frac{1-Z^i}{1+Z^i},\ a_4^i = \frac{2Z^i}{1+Z^i},$$

where we denote the relative magnitude of the impedance as

$$Z^i = \frac{c_\xi^i}{J^i G^i} \Big/ \frac{c_\xi^{i+1}}{J^{i+1} G^{i+1}} \tag{21}$$

Note the meaning of these boundary conditions as reflections of incoming waves from both sides, as they are split into an upward and a downward traveling wave. In the case of the same material being used at both sides of the discontinuity,

the coefficient Z^i can be simplified as the only change is the polar moment of inertia. The other boundary conditions read

$$\alpha^1(t,0) = -\beta^1(t,0) + 2\omega_{TD}(t), \tag{22}$$
$$\beta^N(t,L) = 2\omega_{DH}(t) - \alpha^N(t,L), \tag{23}$$
$$\dot{\omega}_{TD}(t) = \frac{1}{I_{TD}}u_T(t) - \frac{J^1G^1}{c_t^1 I_{TD}}(\omega_{TD}(t) - \beta^1(t,0)), \tag{24}$$
$$\dot{\omega}_{DH}(t) = \frac{J^NG^N}{c_t^N I_{BHA}}(\alpha^N(t,L) - \omega_{DH}) - \frac{1}{I_{BHA}}d(t), \tag{25}$$

To avoid useless case distinctions for the first subsystem and the last one, we will use the following conventions

$$\alpha^0(t,0) = \omega_{TD}, \quad \beta^{N+1}(t,L) = \omega_{DH}, \tag{26}$$
$$a_1^0 = 2,\ a_2^0 = -1,\ a_3^0 = 0,\ a_4^0 = \frac{J^1G^1}{c_t^1 I_{TD}}, \tag{27}$$
$$a_1^N = \frac{J^NG^N}{c_t^N I_{BHA}},\ a_2^N = 0,\ a_3^N = -1,\ a_4^N = 2. \tag{28}$$

We will also denote $t_i = \frac{x_i - x_{i-1}}{c_t^i}$ as the transport time on the i^{th} junction.

F. CONTROL OBJECTIVE AND SPECIFICATIONS

The main control objective of this paper is to regulate the downhole angular velocity at the start-up of a drilling operation (e.g. after a connection) while avoiding entering a stick slip limit cycle. More precisely, we aim to track a given reference trajectory. The control input corresponds to the top-drive motor torque. The resulting system corresponds to an ODE-PDE-ODE configuration where the top-drive ODE is actuated. Note that the configuration would be slightly simpler (PDE-ODE) if we could control the top-drive angular velocity. In the case of the change of set-points, to construct reference trajectories for the downhole angular velocity ω_{DH} that are both smooth, and have vanishing derivatives at the end and start points, we used a semi-analytical function (mollifier). As suggested in [28], we use the integral of the "bump" function as a smooth approximation of the step function with vanishing derivatives. We will denote $m(t)$ such a mollifier function. It is defined by

$$m(t) = \int_0^1 \phi(s-1)ds, \tag{29}$$

where the bump function $\phi(t)$ is defined by

$$\phi(t) = \begin{cases} \dfrac{\exp\left(-\frac{1}{1-t^2}\right)}{\int_{-1}^{1}\exp\left(-\frac{1}{1-\xi^2}\right)d\xi} & \text{for } t \in (-1,1), \\ 0 \quad \text{otherwise,} \end{cases} \tag{30}$$

This mollifier is used to design reference trajectories for the downhole RPM, by choosing an amplitude A_m, switching time t_{sd}, and switching duration t_{sr}:

$$\omega_{ref} = A_m m\left(\frac{t - t_{sd}}{t_{sr}}\right). \tag{31}$$

Note that if the reference trajectory is already a smooth function, there is no need to use the mollifier, whose main purpose is to avoid brutal changes of the reference signal. An alternative way to design the reference signal could be to consider it as the output of a regular exogenous system [48].

The control objective consists in tracking this reference trajectory, i.e. we want $\omega_{DH} \to \omega_{ref}$. In this paper, we present several methodologies for the regulation of the downhole angular velocity. The different algorithms we propose feature specific advantages and limitations. They will be compared with respect to standard criteria that are listed below: overshoot, existence and amplitude of residual oscillations, convergence time, computational effort, simplicity of the controller structure. In what follows, we introduce the control strategies in increasing inherent design complexity.

Below, we summarize the main ideas behind the three proposed approaches and detail their corresponding requirements, limitations and performance w.r.t the proposed criteria. These performances have been evaluated by a series of field case simulations described in Section VIII.

1) **ZTorque and feed-forward controller.** A feedforward controller which can easily be added to the standard industry ZTorque feedback controllers without disturbing the closed-loop behavior has been proposed in [28]. The proposed control law conforms to the 3DOF controller architecture [49] since it has three components: a feedback term, a feedforward term (exploiting the model's differential flatness [50]), and a disturbance cancellation term. However, such a control law has been designed for a single-sectional drillstring (with a lumped BHA) and cannot be straightforwardly extended to multi-sectional drilling devices. In particular, the estimation procedure for $d(t)$ needs to be modified. The revised version of this algorithm is given in Section III.
   - **Requirements:** Knowledge of top-drive torque, estimation of the disturbance term (at least disturbance magnitude).
   - **Limitations:** No rigorous proof of convergence.
   - **Performance:** State-of-the art controller. The feedforward component and the disturbance compensation term considerably reduce the residual oscillations. Possible overshoot and relatively long convergence time due to the oscillations. Simple to implement with a low computational effort.
2) **Multiplicity Induced Dominancy Controller.** In this procedure, we consider the transfer function between the downhole angular velocity and the actuator. This transfer function corresponds to a time-delay system for which we can design a control law that guarantees the placement of the dominant root in the complex plane (and consequently the stability of the closed-loop system). This algorithm is presented in Section IV.
   - **Requirements:** Estimation of the downhole angular velocity, estimation of the disturbance terms.

- **Limitations:** Requires derivative terms, no rigorous proof if more that one section.
- **Performance:** Slight overshoot and oscillations. Low computational effort. Sensitivity to noise (due to the derivation) that may be reduced using a low-pass filter.

3) **Recursive dynamics interconnection framework.** In this procedure, we consider the different sections of the pipe independently. For each section, we find the virtual input that stabilizes the section and guarantees that the output converges towards the virtual input of the next subsystem. The virtual input of the last subsystem (downhole ODE) is chosen to guarantee the tracking of the reference signal. This approach transforms the complex tracking problem into simple interconnected control problems. It is described in Section V
   - **Requirements:** Estimation of the disturbance term, estimation of the states at the junctions, predictions of these states.
   - **Limitations:** Inversion of the ODE dynamics that creates a non-strictly proper control law, thus implying some robustness issues. May be overcome by combining the control law with a low-pass filter. Computational effort.
   - **Performance:** Fast convergence without any residual oscillations. Instantaneous high control effort (mostly due to the compensation of the disturbance). Complex control algorithm with an important computational effort (due to the use of predictors). Robustness is guaranteed by the use of low-pass filter.

The performance and requirements of these three different procedures are summarized in Table 2. A more detailed analysis is proposed in Section VIII. All three procedures require the knowledge of the disturbance term induced by the Coulomb friction terms. Moreover, the two last algorithms require real-time estimation of the state. A state-estimation procedure is proposed in Section VII.

III. SOFTTORQUE, ZTORQUE AND FEED-FORWARD TRACKING

A. PRESENTATION OF THE CONTROLLER

Most of the controllers used in industrial applications correspond to high gain PI controllers and ensure rapid tracking of the top drive set point [51]. Although simple to implement and easy to analyze, these control laws may present aggressive behavior and do not always handle well changes of set-points (generating significant oscillations). Moreover, they cannot compensate the disturbance term $d(t)$ and avoid stick-slip. The current industry standard in handling torsional vibrations are the two products NOV's SoftSpeed [21], [52] and Shell's SoftTorque [22], [26]. In these solutions, the main objective is to reduce the reflection coefficient at the top drive in a particular key frequency range [51]. The main advantage of the ZTorque solution (compared to SoftTorque) relies on the measurement of the torque between the drillstring and top drive, which allows the user to minimize the reflection coefficient of the top drive for a broader range of frequencies. All in all, this feedback control law "artificially" has the top-drive match the impedance of the drill-pipe, $\zeta = J\sqrt{G\rho}$. The block diagram of the ZTorque control law is given in Fig 3. The control signal has the following structure

$$u_T^C = -(C \star (\omega_{SP} - \omega_{TD})), \tag{32}$$

where ω_{SP} is the reference set point for the top-drive angular velocity. Obviously the set point depends on the reference signal we want to track. Moreover, tracking a reference signal implies adding a feed-forward term u_T^F to the stabilizing term u_T^C.

Compared to a simple PI control law, ZTorque also requires measurement of the torque acting from the drillstring on the top drive to work effectively. Thus, it may be necessary to combine the control algorithm with an estimation procedure (state-observer). Even in the absence of a specific disturbance rejection procedure, the ZTorque control law effectively removes stick-slip oscillations at the costs of delivering high instantaneous torque (both positive and negative, which are required to nearly instantaneously overcome top drive motor inertia, field measurements have shown that pipe torque is never negative) to the top drive to allow for impedance matching through rapid velocity changes and a significantly slower response in rotational velocity of the top-drive [53]. However, as shown in [28], it may be relevant to compensate the disturbance term $d(t)$ to avoid undesirable oscillations. Thus, the control design is done in two steps: we first find the top-drive reference signal that corresponds to the downhole reference trajectory we aim to track. This is done using the flatness properties of the system. This reference signal also induces a feed-forward term u_T^F that is added to the stabilizing term u_T^C. Next, we compensate the disturbance. These two steps can be done separately using the superposition principle.

B. LAPLACE ANALYSIS AND DERIVATION OF THE TRACKING COMPONENT

We aim to express the top-drive velocity and control input as functions of the downhole reference velocity. In other words, we are looking for the transfer function between the downhole angular velocity and the control input. To simplify the computations, we will use the Laplace transform. We denote s the Laplace variable. Provided it is defined, the Laplace transform of a function f will be denoted $\hat{f}$. Note that the computations in the Laplace domain that we present below will be used to design the MID controller in the next section. Consider the i^{th} subsystem: from equations (19) and (20), we obtain

$$\begin{pmatrix} a_1^i & 0 \\ -a_3^i & 1 \end{pmatrix} \begin{pmatrix} \alpha^i(t,x_i) \\ \beta^i(t,x_i) \end{pmatrix} = \begin{pmatrix} 1 & -a_2^i \\ 0 & a_4^i \end{pmatrix} \begin{pmatrix} \alpha^{i+1}(t,x_i) \\ \beta^{i+1}(t,x_i) \end{pmatrix}.$$

Controller	Requirements	Performance
ZTorque +feedforward	Top-drive torque Estim. dist. magnitude	Overall good perf. but Residual oscillations + overshoot Slow convergence Low computational effort Simple control architecture
MID	Estim. DH velocity Estim. disturbance	Slight overshoot/residual oscillations Low computational effort Sensitive to noise (derivative term)
Recursive Procedure	Estim. disturbance Estim. states Prediction of the states	Excellent performance No overshoot nor oscillations High instantaneous torque High computational effort Complex control architecture

FIGURE 2: Comparison of the requirements and performance for the three proposed procedures

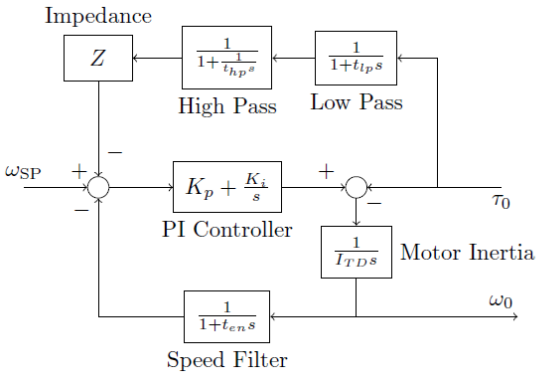

FIGURE 3: Control diagram for a ZTorque system with direct pipe torque measurement. For ZTorque $Z = \frac{1}{\zeta}$ is used. If $Z = 0$, the control diagram is equivalent to a SoftTorque or stiff speed controller system (figure from [28]).

It gives

$$\begin{pmatrix}\alpha^i(t,x_i)\\ \beta^i(t,x_i)\end{pmatrix} = \frac{1}{a_1^i}\begin{pmatrix}1 & -a_2^i\\ a_3^i & -a_2^i a_3^i + a_4^i a_1^i\end{pmatrix}\begin{pmatrix}\alpha^{i+1}(t,x_i)\\ \beta^{i+1}(t,x_i)\end{pmatrix} = D_i\begin{pmatrix}\alpha^{i+1}(t,x_i)\\ \beta^{i+1}(t,x_i)\end{pmatrix},$$

Using the transport structure of equations (17)-(18) and taking the Laplace transform, we obtain for $i < N$

$$\begin{pmatrix}\hat\alpha^i(s,x_{i-1})\\ \hat\beta^i(s,x_{i-1})\end{pmatrix} = \begin{pmatrix}\mathrm{e}^{t_i s} & 0\\ 0 & \mathrm{e}^{-t_i s}\end{pmatrix}\begin{pmatrix}\hat\alpha^i(s,x_i)\\ \hat\beta^i(s,x_i)\end{pmatrix} = \bar D_i(s)\begin{pmatrix}\hat\alpha^{i+1}(s,x_i)\\ \hat\beta^{i+1}(s,x_i)\end{pmatrix}, \tag{33}$$

We also have

$$\begin{pmatrix}\hat\alpha^N(s,x_{N-1})\\ \hat\beta^N(s,x_{N-1})\end{pmatrix} = \begin{pmatrix}\mathrm{e}^{t_N s} & 0\\ 0 & \mathrm{e}^{-t_N s}\end{pmatrix}\begin{pmatrix}1 & 0\\ -1 & 2\end{pmatrix}\begin{pmatrix}\hat\alpha^N(L)\\ \hat\omega_{DH}(s)\end{pmatrix},$$

Taking the Laplace transform of the downhole ODE (25), we obtain

$$\hat\omega_{DH}(s) = \frac{a_1^N}{s + a_1^N}\hat\alpha^N(s,L),$$

which gives

$$\begin{pmatrix}\hat\alpha^N(x_{N-1})\\ \hat\beta^N(x_{N-1})\end{pmatrix} = \begin{pmatrix}\mathrm{e}^{t_N s} & 0\\ 0 & \mathrm{e}^{-t_N s}\end{pmatrix}\begin{pmatrix}1 & 0\\ -1 & 2\end{pmatrix}\begin{pmatrix}\frac{s+a_1^N}{a_1^N}\\ 1\end{pmatrix}\hat\omega_{DH} = \bar D_N(s)\hat\omega_{DH}(s). \tag{34}$$

The top-drive boundary condition (23) rewrites

$$\hat\omega_{TD}(s) = \begin{pmatrix}\frac12 & \frac12\end{pmatrix}\begin{pmatrix}\hat\alpha^1(s,0)\\ \hat\beta^1(s,0)\end{pmatrix}. \tag{35}$$

Thus, we obtain

$$\hat\omega_{TD}(s) = \frac12\begin{pmatrix}1 & 1\end{pmatrix} D(s)\hat\omega_{DH}(s), \tag{36}$$

where the matrix $D(s)$ is defined as

$$D(s) = \bar D_1(s)\bar D_2(s)\dots\bar D_N(s).$$

From (24), we obtain

$$\begin{aligned}\hat u_T(s) &= I_{TD}(s + a_4^0)\omega_{TD} - a_4^0\beta^1(s,0)\\ &= \frac12(I_{TD}(s+a_4^0),\ I_{TD}(s+a_4^0) - 2a_4^0)D(s)\hat\omega_{DH}(s)\\ &= A(s)\hat\omega_{DH}(s),\end{aligned} \tag{37}$$

where

$$A(s) = \frac12(I_{TD}(s + a_4^0),\ I_{TD}(s+a_4^0) - 2a_4^0)D(s)\hat\omega_{DH}(s).$$

This corresponds to the transfer function between the input and the state ω_{DH}. Thus, if we consider a downhole reference angular velocity $\omega_{ref}(t)$, the corresponding feed-forward tracking contribution to the top drive set-point will be defined by

$$\hat\omega_{SP}(s) = D(s)\hat\omega_{ref}(s), \tag{38}$$

and the actuation contribution term as

$$\hat u_T^F(s) = A(s)\hat\omega_{ref}(s). \tag{39}$$

This feed-forward control term u_T^F is added to the stabilizing control term u_T^C in the ZTorque control law to ensure trajectory tracking.

C. DISTURBANCE CANCELLATION-SWITCHING MODE PROCEDURE

A procedure was proposed in [28] to compensate for the effect of the disturbance term $d(t)$. In this procedure, the disturbance was assumed to take the form of a Heaviside step function acting the instant the BHA releases from the stick phase. The value of the disturbance term was either computed using the torque and drag model directly (see equation (10)) or by computing the changes in motor torque induced by the stick-slip oscillations. However, these two methods cannot be straightforwardly extended to the case of a multi-sectional drillstring (due to the multiple reflection nodes). It is essential to emphasize that the disturbance term becomes constant once the BHA releases from the stick phase, since in that case, the function $\mathcal{F}$ defined by (4) only depends on the spatial variable x (and consequently its integral is constant). A constant disturbance term becomes much simpler to estimate and compensate accurately. It is possible to envision a switching mode control law to reduce the performance limitations related to a wrong estimation of the disturbance term. In the first mode, we impose an arbitrary constant value (large enough) as the control input reference to guarantee the BHA release from the stick phase. Once this has been done, we switch to the second mode, where we can consider the disturbance term d as a constant and compensate for it. It is then possible to add a compensation term in the control input to eliminate the constant disturbance term. The compensation procedure will be given in Section VI. This disturbance rejection term will be directly added to the control input (due to the superposition principle). All the controllers will be based on the same switching-mode procedure disturbance rejection procedure as we aim to compare the nominal performance without the stick-slip oscillations.

IV. NEUTRAL-TYPE MODEL FOR THE TORSIONAL OSCILLATIONS

In this section, we consider a low complexity control design that is inspired from [33], [54] and is based on the *multiplicity induced-dominancy* (MID). We first rewrite $\omega_{DH}(t)$ as the solution of a neutral-type equation that depends on the control input u_T, thus relating the system variables at both ends of the drilling rod. We can show that there is a one-to-one correspondence between the solutions of the mixed problem for hyperbolic PDE and the initial value problem for the associated system of functional equations [55]. We will neglect the disturbance term in the design of the control law since this term can be canceled using the procedure described in Section VI.

A. NEUTRAL FORMULATION AND LOW COMPLEXITY CONTROLLER DESIGN

The first step before applying the MID procedure consists in rewriting the PDE system as a time-delay system. To simplify the computations, we will use the Laplace analysis presented in the previous section. Following the approach of [33], [54], we can reduce (37) to an I/O system of neutral type. Let us define $\Delta(s)$ as

$$\Delta(s) = \Pi_{i=1}^{N} \mathrm{e}^{-t_i s} = \mathrm{e}^{-t_{tot} s}.$$

Multiplying equation (37) by $\Delta(s)$, we can remove all the positive-delay exponential terms (i.e. the terms $\mathrm{e}^{t_i s}$). Using the Laplace transform, we can rewrite equation (37) as a quasipolynomial including multiple delays:

$$\mathrm{e}^{-t_{tot} s} \hat{u}_T(s) = L(s) \hat{\omega}_{DH}(s), \tag{40}$$

where the function L is defined by

$$\begin{cases} L(s) = P(s) + \sum_{i=1}^{N+1} Q_i(s) e^{-s\delta_i}, \\ P(s) = \sum_{k=0}^{N+1} a_k s^k, \quad Q_i(s) = \sum_{k=0}^{N+1} b_{ik} s^k, \end{cases} \tag{41}$$

where the δ_i are positive delays corresponding to (partial) sums of t_i and where the a_k, b_{ik} are real coefficients. In the sequel, we apply the MID property to design a reduced-order controller thanks to the delayed action of the angular position, angular speed, and angular acceleration.

B. MID-CONTROLLER FOR A SINGLE-SECTION DRILLSTRING

In this section we consider the case $N = 1$ (case of a drillstring composed of an unique pipe). The objective is to show how to apply the MID procedure on a simple case. Equation (37) considerably simplifies as after a multiplication by $2\mathrm{e}^{-t_{tot} s}$, it rewrites as a *neutral equation of order 2*:

$$\begin{aligned} 2\mathrm{e}^{-t_{tot} s} \hat{u}_T(s) = (&\frac{J^1 G^1}{c_t^1} + (I_{BHA} + I_{TD})s + \frac{c_t^1}{J^1 G^1} I_{BHA} \\ I_{TD} s^2) \hat{\omega}_{DH}(s) - (&\frac{J^1 G^1}{c_t^1} - (I_{BHA} + I_{TD})s \\ + \frac{c_t^1}{J^1 G^1} I_{BHA} I_{TD} s^2) &\mathrm{e}^{-2t_{tot} s} \hat{\omega}_{DH}(s). \end{aligned} \tag{42}$$

Proposition 1: Consider Equation (42) with the control law given by:

$$\hat{u}_T(s) = -\left(\alpha_0 + \alpha_1 s + \alpha_2 s^2\right) e^{(-t_{tot} s)} \hat{\omega}_{DH}(s). \tag{43}$$

If the polynomial

$$\begin{aligned} R(Z) = &3\mathrm{I}_{BHA} (c_t^1)^4 \mathrm{I}_{TD} + 3\mathrm{I}_{BHA} G^1 J^1 {c_t^1}^2 x_1 + 3\mathrm{I}_{TD} G^1 J^1 \\ &(c_t^1)^2 x_1 + 2(G^1)^2 {J^1}^2 x_1^2 + (6\mathrm{I}_{BHA} \mathrm{I}_{TD} (c_t^1)^2 + 2\mathrm{I}_{BHA} G^1 \\ &J^1 x_1 + 2\mathrm{I}_{TD} G^1 J^1 x_1) Z + 2\mathrm{I}_{BHA} \mathrm{I}_{TD} Z^2 \end{aligned} \tag{44}$$

admits two roots $Z_2 < Z_1 < 0$ then the following tuning

$$\begin{cases} \alpha_0 = \dfrac{q_0\,\mathrm{e}^{\frac{2s_0x_1}{c_t^1}} + 2\mathrm{I}_{BHA}\mathrm{I}_{TD}G^{1\,2}J^{1\,2}c_t^{1\,2}x_1^2}{4\mathrm{I}_{BHA}c_t^{1\,3}\mathrm{I}_{TD}G^1J^1x_1^2}, \\ \alpha_1 = \dfrac{q_1\,\mathrm{e}^{\frac{2s_0x_1}{c_t^1}} - G^1J^1x_1c_t^{1\,2}\left(\mathrm{I}_{TD}+\mathrm{I}_{BHA}\right)}{2G^1J^1x_1c_t^{1\,2}}, \\ \alpha_2 = \dfrac{\left(\left(2s_0x_1c_t^1+2c_t^{1\,2}\right)\mathrm{I}_{TD}+G^1J^1x_1\right)\mathrm{I}_{BHA}+\mathrm{I}_{TD}G^1J^1x_1}{2c_t^1G^1J^1\mathrm{e}^{-\frac{2s_0x_1}{c_t^1}}} \\ \qquad + \dfrac{\mathrm{I}_{BHA}\mathrm{I}_{TD}c_t^{1\,2}}{2c_t^1} \end{cases} \tag{45}$$

where

$$\begin{aligned} q_0 =& 2((21s_0x_1c_t^{1\,4}+\frac{27}{2}c_t^{1\,5})\mathrm{I}_{TD}^2+6x_1G^1(s_0x_1+\frac{5c_t^1}{2})J^1c_t^{1\,2}\\ &\mathrm{I}_{TD}+G^{1\,2}J^{1\,2}x_1^2(s_0x_1+\frac{3c_t^1}{2}))c_t^1\mathrm{I}_{BHA}^2+12x_1G^1(c_t^{1\,3}(s_0x_1\\ &+\frac{5c_t^1}{2})\mathrm{I}_{TD}^2+\frac{11\mathrm{I}_{TD}G^1J^1c_t^{1\,2}x_1}{6}+\frac{G^{1\,2}J^{1\,2}x_1^2}{6})J^1\mathrm{I}_{BHA}\\ &+2x_1^2\left(c_t^1(s_0x_1+\frac{3c_t^1}{2})\mathrm{I}_{TD}+G^1J^1x_1\right)G^{1\,2}\mathrm{I}_{TD}J^{1\,2},\\ q_1 =& 2\left((6s_0x_1c_t^{1\,2}+\frac{9}{2}c_t^{1\,3})\mathrm{I}_{TD}+G^1J^1x_1(s_0x_1+4c_t^1)\right)\\ &c_t^1\mathrm{I}_{BHA}+2x_1G^1\left(c_t^1\left(s_0x_1+4c_t^1\right)\mathrm{I}_{TD}+2G^1J^1x_1\right)J^1,\\ \rho =& \frac{4s_0x_1c_t^1\mathrm{I}_{BHA}\mathrm{I}_{TD}+6\mathrm{I}_{BHA}\mathrm{I}_{TD}c_t^{1\,2}+2\mathrm{I}_{BHA}G^1J^1x_1}{\mathrm{I}_{BHA}\mathrm{I}_{TD}c_t^{1\,2}}\\ &+\frac{2\mathrm{I}_{BHA}G^1J^1x_1+2\mathrm{I}_{TD}G^1J^1x_1}{\mathrm{I}_{BHA}\mathrm{I}_{TD}c_t^{1\,2}},\\ &\text{satisfying}\quad 2\sqrt{3}<\rho<4, \end{aligned}$$

is a stabilizing design which ensures the assignment of the closed-loop rightmost root at the quadruple root at $s_0 = Z_1/(c_t^1\,x_1)$, which corresponds to the exponential decay of the closed-loop system's solution.

The proof of Proposition 1 relies on a result from [31] where a systematic design of the classical PID controller able to stabilize delayed first-order plants is proposed (see also [34] for a more detailed proof).

Proof 1: The closed-loop characteristic function corresponding to (42) and (43) writes:

$$\begin{aligned} L(s) =& ((-\frac{\mathrm{I}_{BHA}c_t^1\mathrm{I}_{TD}}{2J^1G^1}+\alpha_2)s^2+(-\frac{-\mathrm{I}_{BHA}G^1J^1c_t^1-\mathrm{I}_{TD}G^1J^1c_t^1}{2c_t^1J^1G^1}\\ &+\alpha_1)s-\frac{J^1G^1}{2c_t^1}+\alpha_0)\mathrm{e}^{-\frac{2sx_1}{c_t^1}}+\frac{\mathrm{I}_{BHA}c_t^1\mathrm{I}_{TD}s^2}{2J^1G^1}\\ &+\frac{\left(\mathrm{I}_{BHA}G^1J^1c_t^1+\mathrm{I}_{TD}G^1J^1c_t^1\right)s}{2c_t^1J^1G^1}+\frac{J^1G^1}{2c_t^1} \end{aligned}$$

Forcing a spectral value to have multiplicity four allows not only the tuning of the controllers gains (45) but also (after the scaling and the normalization $z = c_t^1(s-s_0)/2\,x_1$) a normalized representation of the quasipolynomial function $\tilde{L}(z) = 4\,x_1^2/c_t^{1\,2}\,L(s)$

$$\begin{aligned} \tilde{L}(z) =& z^2+(\rho-6)\,z-3\,\rho+12+[\left(\frac{\rho}{2}-1\right)z^2\\ &+(2\,\rho-6)\,z+3\,\rho-12]\mathrm{e}^{-z}. \end{aligned} \tag{46}$$

where $\rho = (4s_0x_1c_t^1\mathrm{I}_{BHA}\mathrm{I}_{TD}+6\mathrm{I}_{BHA}\mathrm{I}_{TD}c_t^{1\,2}+2\,\mathrm{I}_{BHA}G^1J^1x_1+2\mathrm{I}_{TD}G^1J^1x_1)/\mathrm{I}_{BHA}\mathrm{I}_{TD}c_t^{1\,2}$.

The value $s = s_0$ is a root of multiplicity 4 of L if and only if $z = 0$ is a root of multiplicity 4 of the normalized quasipolynomial $\tilde{L}$, i.e., the dominance of s_0 as a root of L is equivalent to the dominance of $z = 0$ as a root of $\tilde{L}$. Next, integrating by parts yields the following integral representation of $\tilde{L}$

$$\tilde{L}(z) = \frac{z^4}{2}\int_0^1 t\,(1-t)\,(t(\rho-4)+2)\,\mathrm{e}^{-tz}\,\mathrm{d}t. \tag{47}$$

It is shown in [34] that under $2\sqrt{3} < \rho < 4$ the integral function (47) has all its roots in the complex left half-plane, which ends the proof.

C. COMMENTS OF THE CASE OF A MULTI-SECTIONAL DRILLING DEVICE

As established in (41), the propagation of the vibration through a multi-sectional drilling device is governed by a multiple delay neutral system.

Although the partial pole placement paradigm for time-delay systems remains restricted to the single delay case, numerical investigations suggest its validity in the case of multiple delay neutral systems. Extending such a design methodology to this case or to the case of distributed delays becomes an interesting theoretical research direction. To the best of the authors' knowledge, the only particular case in such a class for which a proof for the MID to hold is the first order retarded equation with two discrete delays, see for instance [56]. Extensions to more general cases will require new ideas and techniques to build the necessary and sufficient conditions for multiple spectral values to be dominant. Here, we will solve the problem numerically, assuming that Proposition 1 extends in this case.

V. RECURSIVE DYNAMICS INTERCONNECTION FRAMEWORK

The last class of controllers we consider in this paper relies on a recursive interconnected dynamics framework. Roughly speaking, the proposed control law is recursively obtained by considering for each subsystem a virtual input that stabilizes it but also guarantees that the subsystem's output converges towards the virtual input of the next subsystem. The virtual input of the last subsystem guarantees the convergence of the ODE state towards the reference signal. This approach has been introduced in [57] and completed in [37] to design output-feedback controllers. It is somehow inspired by the original philosophy of the backstepping methodology [58]. Let us first introduce the following terminology

Definition 1: For a subsystem i, we denote $\hat{V}_i(t)$ the action of the $(i-1)^{th}$ subsystem on this subsystem. This function will be called ***virtual input*** acting on the i^{th} subsystem. We also denote $\chi_i(t)$ the action of the $(i+1)^{th}$ subsystem on the i^{th} subsystem. This function will be called ***virtual disturbance*** acting on the i^{th} subsystem.

These different notations are summarized in Figure 4. With these notations, we have, for instance, $\hat{V}_2(t) = a_1^1\alpha^1(t, x_1)$, $\chi_2(t) = a_3^2\beta^3(t, x_2)$.

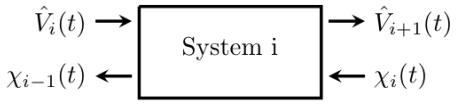

FIGURE 4: Schematic representation of the interactions between the different subsystems

In the proposed procedure, each subsystem is stabilized using its leftward neighbor. Again, we neglect the disturbance term in the design of the control law for the moment since this term can be canceled using the procedure described in Section VI.

A. DOWNHOLE ODE

Let us consider the downhole ODE (25). For this equation, the virtual input $\hat{V}_{N+1}$ corresponds to $\alpha^N(t, L)$ (i.e. the value of the Riemann invariant α^N evaluated at $x = L$). It rewrites

$$\dot{\omega}_{DH}(t) = \hat{V}_{N+1}(t) - a_1^N\omega_{DH}(t) - \frac{1}{I_{BHA}}d(t).$$

Then, it is sufficient to choose $\hat{V}_{N+1}(t)$ as

$$\begin{aligned}\hat{V}_{N+1}(t) =&\dot{\omega}_{ref}(t) + a_1^N\omega_{ref}(t)\\ &- K_D(\omega_{DH}(t) - \omega_{ref}(t)),\end{aligned} \tag{48}$$

where K_D is a positive constant.

B. OUTPUT TRACKING FOR THE PDES SUBSYSTEMS

Consider now the i^{th}-subsystem (17)-(18). We have

$$\alpha^i(t, x_i) = \hat{V}_i(t - t_i) + a_2^i\beta^i(t - t_i, x_{i-1}),$$

and we want $a_1^{i+1}\alpha^i(t, x_i)$ to track $\hat{V}_{i+1}(t)$. Thus, we can choose

$$\hat{V}_i(t) = \frac{1}{a_1^{i+1}}(\hat{V}_{i+1}(t + t_i) - a_2^i\beta^i(t, x_{i-1})), \tag{49}$$

to guarantee the tracking of the reference control signal $\hat{V}_{i+1}$.

C. OUTPUT TRACKING FOR THE TOP-DRIVE ODE

Consider now the top-drive ODE (24). We want the signal $2\omega_{TD}$ to track $\hat{V}_0(t)$. Then, we can choose u_T as

$$\begin{aligned}u_T(t) =&\frac{I_{TD}}{2}(-a_4^0\beta^1(t, 0) + \dot{\hat{V}}_1(t) + a_4^0\hat{V}_1(t)\\ &- K_0(\omega_{TD} - \hat{V}_1(t)).\end{aligned} \tag{50}$$

The control u_T guarantees the tracking of the reference downhole angular velocity.

The control law (50) features several important drawbacks

1) It requires the knowledge of future values of the PDE states and of the downhole ODE state.
2) The inversion of the ODE dynamics may result to a non-strictly proper control law, thus implying some robustness issues.

To overcome these limitations, we will design an observer-predictor that can provide future values of the different states of the system. This will be done in Section VII. To obtain a strictly proper control law (thus guaranteeing admissible robustness margins), it is possible to low-pass filter the non-strictly proper terms that appear in the control input u_T (see [59] or [60, Chapter 7] for instance). Provided that the low-pass filter is well-tuned, we can guarantee the tracking of the reference signal with a strictly proper controller.

Remark 2: In the case of a uni-sectional drilling device (with a lumped BHA), the control law (50) does not require the prediction of the downhole ODE state when choosing $K_D = 0$ (since the downhole ODE is naturally exponentially stable).

VI. DISTURBANCE REJECTION

In this section, we propose a procedure to eliminate the effect of the disturbance term $d(t)$. Following the switching-mode strategy presented in Section III-C, we can consider this disturbance as a constant. It now becomes possible to adjust the recursive methodology presented in Section V to eliminate the disturbance. Indeed, define for all i

$$\hat{V}_{N+1}^d(t) = \frac{d}{I_{BHA}}, \tag{51}$$

$$\hat{V}_i^d(t) = \frac{1}{a_1^{i+1}}(\hat{V}_{i+1}^d(t + t_i) - a_2^i\beta^i(t, x_{i-1})), \tag{52}$$

$$\begin{aligned}u_T^d(t) =& \frac{I_{TD}}{2}(-a_4^0\beta^1(t, 0) + \dot{\hat{V}}_1^d(t) + a_4^0\hat{V}_1^d(t)\\ &- K_0(\omega_{TD} - \hat{V}_1^d(t)).\end{aligned} \tag{53}$$

The control input u_T^d can be seen as a disturbance rejection term. It can be added to the different controllers due to the superposition principle.

VII. STATE ESTIMATION AND OUTPUT-FEEDBACK CONTROL

Simple control algorithms (as PID controllers) directly use the available measurements to design a stabilizing control input. However, more complex control procedures may require a real-time estimation of the distributed states all over the drillstring. The incentive to do so, rather than relying on simple controllers, is a performance criterion: explicitly taking into account the delays and high-frequency content in the design of the controller should lead to overall increased performance for the chosen specifications. Thus, it may be necessary to design a 'soft-sensor' (observer) that combines measurements from physical sensors (here the top drive angular velocity $\omega_{TD}(t)$) with the model of the system dynamics to provide estimates of the states. It combines 'open-loop' terms (based on the equations describing the evolution of the system) and 'closed-loop' terms (output injection gains) that correct the dynamics based on the error between the estimated output and the measured one.

An adaptive soft sensor has been proposed in [40] for the case of a single-sectional drillstring (a lumped approximation was used for the collar section and the BHA). The observer was based on a backstepping methodology inspired by [61]. This observer guarantees fast and robust convergence of the estimates. Moreover, it is adaptive in that it estimates the side forces and updates the observer model kinetic or static friction factor iteratively. However, it cannot estimate the transition velocity ω_c (which might limit its performance).

Here, we present a different type of state-observer, which is based on our recursive dynamics framework. It can be seen that a system i will act on the subsystem $i+1$ through $\alpha^i(t,x_i)$, and on the subsystem $i-1$ through $\beta^i(t,x_{i-1})$. Then, going recursively from one subsystem to the next, we can estimate the states at each subsystem's boundaries. However, due to the system's natural inertia (induced by the transport phenomenon in the PDEs), there are some delays in the estimations. More precisely, we can only estimate past values of the boundary states. It is then possible to apply similar predictors to those designed in [37] to obtain non-delayed estimations. Such an approach (that combines delayed estimations and state-predictions) is similar to the one used for finite-dimensional systems [62].

A. BOUNDARY STATE ESTIMATION

Since equations (17)-(18) are transport equations, it is possible to express the states $\alpha^i(t,x)$ and $\beta^i(t,x)$ as functions of the boundary states. Indeed, we have for all $x\in[x_{i-1},x_i]$

$$\begin{aligned}\alpha^i(t,x)&=\alpha^i(t-\frac{x-x_{i-1}}{c_t^i},x_{i-1})\\&=a_1^{i-1}\alpha^{i-1}(t-\frac{x-x_{i-1}}{c_t^i},x_{i-1})\\&+a_2^{i-1}\beta^i(t-\frac{x-x_{i-1}}{c_t^i},x_{i-1}),\end{aligned}\tag{54}$$

$$\begin{aligned}\beta^i(t,x)&=\beta^i(t-\frac{x_i-x}{c_t^i},x_i)=a_4^i\beta^{i+1}(t-\frac{x_i-x}{c_t^i},x_i)\\&+a_3^i\alpha^i(t-\frac{x_i-x}{c_t^i},x_i).\end{aligned}\tag{55}$$

Thus, it is sufficient to estimate the boundary states $\alpha^i(t,x_i)$ and $\beta^i(t,x_{i-1})$ to obtain an estimation of the distributed states (α^i,β^i). We have the following Lemma.

Lemma 1: Consider $i\in[1,N]$ and assume that $\alpha^{i-1}(t,x_{i-1})$, $\beta^i(t,x_{i-1})$ are known on the time interval $[t,t+t_i]$. Then, there exist two linear operators $\mathcal{L}_{\alpha^i}$ and $\mathcal{L}_{\beta^i}$, such that

$$\begin{aligned}\alpha^i(t,x_i)&=\mathcal{L}_{\alpha^i}(\alpha^{i-1}(\cdot,x_{i-1}),\beta^i(\cdot,x_{i-1})),\\\beta^{i+1}(t,x_i)&=\mathcal{L}_{\beta^i}(\alpha^{i-1}(\cdot,x_{i-1}),\beta^i(\cdot,x_{i-1})).\end{aligned}$$

Proof 2: Using the method of characteristics, we immediately obtain

$$\begin{aligned}\alpha^i(t,x_i)&=\alpha^i(t-t_i,x_{i-1})=a_1^{i-1}\alpha^{i-1}(t-t_i,x_{i-1})\\&+a_2^{i-1}\beta^i(t-t_i,x_{i-1}),\end{aligned}\tag{56}$$

$$\begin{aligned}\beta^{i+1}(t,x_i)&=\frac{1}{a_4^i}\beta^i(t+t_i,x_{i-1})-\frac{a_3^ia_2^{i-1}}{a_4^i}\beta^i(t-t_i,x_{i-1})\\&-\frac{a_3^ia_1^{i-1}}{a_4^i}\alpha^{i-1}(t-t_i,x_{i-1}).\end{aligned}\tag{57}$$

This gives the operators $\mathcal{L}_{\alpha^i}$ and $\mathcal{L}_{\beta^i}$.

This Lemma expresses the fact that knowing the boundary states $\alpha^{i-1}(t,x_{i-1}),\beta^i(t,x_{i-1})$ at time t, it becomes possible to estimate the boundary states $\alpha^i(t,x_i),\beta^{i+1}(t,x_i)$ at time $t-t_i$. Thus, knowing the states $\beta^1(t,0)$ and $\omega_{TD}(t)$, it becomes possible to estimate delayed values of the PDE states and of the downhole ODE state ω_{DH} (using equation (23)), the value of the delay depending of the considered subsystem. As the state ω_{TD} corresponds to the measurement, it is already known (as well as its delayed values). However the state $\beta^1(s,0)$ (or its delayed values) remains unknown. From equation (24), we have

$$\beta^1(t,0)=\frac{c_t^1I_{TD}}{J^1G^1}(\dot\omega_{TD}(t)-\frac{1}{I_{TD}}u_T(t))+\omega_{TD}(t),\tag{58}$$

which gives us the value of $\beta^1(t,0)$. However, this estimation requires differentiating the output signal ω_{TD}, which may amplify potential noise. From a control point of view, this problem can be avoided by coupling the control law with a well-tuned low-pass filter (as explained in [59] or [60, Chapter 7]) to still fulfill the stabilization objective. Recursively applying Lemma 1, we can obtain delayed estimations of the states $\alpha^i(t,x_i)$ and $\beta^{i+1}(t,x_i)$ (the corresponding delays being $\sum_{j=1}^i t_j$). More precisely, we define the *t_{tot}-delay operator* $\bar{\cdot}$ such that for any function γ, we have

$$\bar\gamma(t)=\gamma(t-t_{tot}),$$

where $t_{tot}=\sum_{i=1}^N t_i$ is the total transport time. We can then define $\hat{\bar\alpha}^i(t,x_i)$ and $\hat{\bar\beta}^{i+1}(t,x_i)$ as the estimations of these t_{tot}-delayed states. Note that these estimations are actually available on a time horizon $[t,t+t_{tot}-\sum_{j=1}^N t_j]$. In what follow, we will combine these estimations with state predictors to compute un-delayed estimations of the states. From these predictions, it will be straightforward to compute the distributed states using equation (55). The design of the predictors will require the knowledge of a (delayed) version of the disturbance $d(t)$, which is possible using equation (10).

B. STATE-PREDICTION

In the previous section, we used our recursive dynamics interconnection framework to estimate delayed values of the PDEs boundary states and of the ODE states as well as the delayed disturbance term. However, to design an output feedback control law for our system, we need to estimate non-delayed values of these boundary states. We now design a predictor for the boundary states $\bar\alpha^i(t,x_i)$ and $\bar\beta^i(t,x_i)$.

The predictor will give $t_{tot} + \sum_{j=1}^{i} t_j$ ahead of time values of these delayed boundary states. Using the method of characteristics, we have

$$\bar{\alpha}^i(t, x_i) = a_1^{i-1}\bar{\alpha}^{i-1}(t - t_i, x_{i-1}) + a_2^{i-1}\bar{\beta}^i(t - t_i, x_{i-1}), \tag{59}$$

$$\bar{\beta}^i(t, x_{i-1}) = a_4^i\bar{\beta}^{i+1}(t - t_i, x_i) + a_3^i\bar{\alpha}^i(t - t_i, x_i). \tag{60}$$

and

$$\dot{\bar{\omega}}_0(t) = \frac{1}{I_{TD}}\bar{u}_T(t) - \frac{J^1G^1}{c_t^1 I_{TD}}(\bar{\omega}_{TD}(t) - \bar{\beta}^1(t, 0)), \tag{61}$$

$$\dot{\bar{\omega}}_{DH}(t) = \frac{J^N G^N}{c_t^N I_{BHA}}(\bar{\alpha}^N(t, L) - \bar{\omega}_{DH}(t)) - \frac{1}{I_{BHA}}\bar{d}, \tag{62}$$

We can then define the functions $P_{\bar{\beta}_i}(t, s)$, $P_{\bar{\alpha}_i}(t, s)$ as the state prediction of future values of $\bar{\beta}_i(t, x_{i-1})$ (resp. $\bar{\alpha}_i(t, x_i)$) ahead a time $t_{tot} + \sum_{j=1}^{i-1} t_j$ (resp $t_{tot} + \sum_{j=1}^{i} t_j$) by the set of equations (63)-(64).

$$P_{\bar{\alpha}_i}(t, s) = \begin{cases} \hat{\bar{\alpha}}_i(s + t_{tot} + \sum_{j=1}^{i} t_j, 1) \\ \text{if } s \in [t - 3t_{tot} - \sum_{j=1}^{i} t_j, t - t_{tot} - \sum_{j=1}^{i} t_j] \\ a_1^{i-1}\bar{P}_{\bar{\alpha}_{i-1}}(t, s) + a_2^{i-1}P_{\bar{\beta}_i}(t, s) \\ \text{otherwise,} \end{cases} \tag{63}$$

$$P_{\bar{\beta}_i}(t, s) = \begin{cases} \hat{\bar{\beta}}_i(s + t_{tot} + \sum_{j=1}^{i-1} t_j, 1) \\ \text{if } s \in [t - 3t_{tot} - \sum_{j=1}^{i-1} t_j, t - t_{tot} - \sum_{j=1}^{i-1} t_j] \\ a_4^i\bar{P}_{\bar{\beta}_{i+1}}(t, s - 2t_i) + a_3^i P_{\bar{\alpha}_i}(t, s - 2t_i) \\ \text{otherwise,} \end{cases} \tag{64}$$

Note that these predictors are well-defined and causal. The right-end of the chain is interconnected with the ODE, described by equation (62). We can also define $P_{\bar{\omega}_{DH}}(t, s)$ (see [63], [64]) as the state prediction of future values of $\bar{\omega}_{DH}$ (ahead a time $\sum_{j=1}^{N} t_j$), for $s \in [t - t_{tot} - \sum_{j=1}^{N} t_j, t]$, by equation (65).

$$P_{\bar{\omega}_{DH}} = \begin{cases} \hat{\bar{\omega}}_{DH}(s + 2t_{tot}) \quad \text{if } s \in [t - 2t_{tot} - \sum_{j=1}^{N} t_j, t - 2t_{tot}] \\ \mathrm{e}^{-\frac{J^N G^N}{c_t^N I_{BHA}} t_{tot}}(\hat{\bar{\omega}}_{DH}(s) + \int_s^{s+t_{tot}} \mathrm{e}^{-\frac{J^N G^N}{c_t^N I_{BHA}}(s-\nu)} \\ (\frac{J^N G^N}{c_t^N I_{BHA}} P_{\bar{\alpha}_N}(t, \nu - t_{tot} + P_d(t, \nu - t_{tot}))d\nu) \\ \text{otherwise.} \end{cases} \tag{65}$$

where the prediction of the disturbance term $P_{\bar{d}}$ is computed using the predictions of the PDE states and equation (10) (expressed in the Riemann coordinates). The explicit expression is not given here for sake of simplicity. From these definitions, we immediately have:

$$P_{\bar{\alpha}_i}(t, s) = \hat{\bar{\alpha}}_i(s + t_{tot} + \sum_{j=1}^{i-1} t_j, 0), \ s \in [t - 2t_{tot} - \textstyle\sum_{j=1}^{i-1} t_j, t],$$

$$P_{\bar{\alpha}_i}(t, s) = \hat{\bar{\alpha}}_i(s + t_{tot} + \sum_{j=1}^{i} t_j, 1), \ s \in [t - 2t_{tot} - \textstyle\sum_{j=1}^{i} t_j, t],$$

$$P_{\bar{\omega}_{DH}}(t, s) = \hat{\bar{\omega}}_{DH}(s + t_{tot} + \sum_{j=1}^{N} t_j), \ s \in [t - 2t_{tot} - \textstyle\sum_{j=1}^{N} t_j, t].$$

Note that there is no need to predict the ODE state $\bar{\omega}_0$ on $[t, t + t_{tot}]$ since it is actually measured. To numerically compute the predictions, we first initialize the predictors using the estimations obtained above. These values are stored in a buffer. Then, it becomes possible to directly use equations (63)-(65) to compute the prediction at the next time step. These predictions of the states can be used to obtain output-feedback versions of the state-feedback control laws introduced in the previous sections. As stated above, they can be coupled with a well-tuned low-pass filter to be strictly proper and avoid the effects of high-frequency noise.

VIII. SIMULATION RESULTS

In this section, we test the performance of our different algorithms against simulated data representing field scenarios. We consider the 2D wellbore profile shown in Figure 5. The well represents a simple build and hold well used throughout the world. It corresponds to an S-Shaped well. More discussion of this synthetic example may be found in [7]. The pipe is made of two sections, whose coefficients are given in Table 5. The static and kinematic friction factors are assumed to be constant along the drillstring. We will consider the performance of the different algorithms in three scenarios that correspond to different lengths for the drilling device (we will denote this length MD) for the wellbore survey pictured in Figure 5. Depending on the choice of MD, different behavior can be expected

- In the first scenario we consider that $MD = 1400m$, which corresponds to the vertical section of the well. Consequently, the effect of the Coulomb friction terms is almost negligible. This case will be referred as the "free drillstring" case.
- In the second scenario, we consider that $MD = 2200m$, which means that the lower part of the drillstring is almost horizontal and is subject to important Coulomb side forces.
- In the last scenario we consider that $MD = 3200m$, which corresponds to the complete S-Shaped well.

In the model's numerical implementation, the wave equation is transformed into transport equations discretized using a first-order upwind scheme. This choice is made to ensure numerical robustness and avoid spurious oscillations, as higher-order schemes perform poorly due to the temporal

TABLE 1: Numerical values of the parameters for the drillstring model in Figure 5.

Param.	Value	Param.	Value
A^1	$0.005\ \text{m}^2$	A^2	$0.0229\ \text{m}^2$
J^1	$2.28 \times 10^{-5}\ \text{m}^4$	J^2	$1.49 \times 10^{-4}\ \text{m}^4$
G^1	6.1×10^{10} m	G^2	6.7×10^{10} m
ρ^1	$7850\ \text{kg/m}^3$	ρ^2	$7850\ \text{kg/m}^3$
x_1	1570 m	L	1700 m
μ_k	0.28	μ_s	0.45
I_{TD}	$2900\ \text{kg.m}^2$	I_{BHA}	$152.9\ \text{kg.m}^2$
ω_c	$1.5\ \text{rads}^{-1}$		

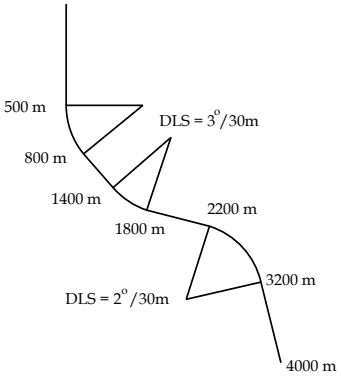

FIGURE 5: Wellbore survey of the well.

discontinuities introduced by the distributed differential inclusions used to represent the Coulomb friction. To guarantee numerical accuracy, we choose a sufficiently fine spatial grid. This is an amenable approach since the simulation speed is not of critical importance for the present analysis (only the computational efforts of the estimation algorithms matter). In all simulations, a spatial grid of 500 cells is used for the drillstring. We choose the time-step such that the Courant-Friedrichs-Lewy (CFL) condition [65] is satisfied. All the simulations are done using MATLAB. This simulation example has been proved to be reliable against field data (see [7]).

A. SCENARIO A: FREE DRILLSTRING

Similarly to what has been done in [28], we initially consider the case of a drillstring spinning freely and neglect the kinematic and static friction terms. The objective is to highlight the respective features of the proposed control strategies. This scenario somehow corresponds to the vertical part of the wellbore pictured in in Figure 5 ($MD = 1400m$). The drillstring is initially at rest, and we first change the setpoint to 120 RPM before going back to 60 RPM. More precisely, the velocity setpoint is changed in two approximate steps according to

$$\omega_{SP} = 120m\left(\frac{t-20}{10}\right) - 60m\left(\frac{t-60}{10}\right). \qquad (66)$$

As the amount of power available to the rig is limited (due to a constraint in on-site generating capacity), we add a torque limitation the actuator. Indeed, on typical AC top drives, torque is proportional to electric current. Thus, a large increase in current may cause a power overload and a large increase in torque may also exceed the torque limits on gearing or other components in the top drive or near- surface rotary equipment. To depict this effect in the proposed simulations, we add a 30 kNm max torque constraint.

We have pictured in Figure 6 the temporal evolution of the top-drive and downhole velocities. We have also plotted the corresponding control efforts (to compare the energy-requirements for each strategy). We see that without the trajectory feed-forward component, the set-point changes induce oscillations that do not vanish (subfigures (a,b)). Among the different control strategies, the recursive algorithm (subfigures (e,f)) presents the smoothest behavior with a reasonable control effort and no overshoot nor oscillations. However, one must keep in mind that this is done at the cost of a higher numerical complexity. The MID algorithm and the feedforward procedure present comparable performance. Note that with the given set of coefficients, the transport delay between the top-drive and the BHA is equal to 0.71s. It explains why the two curves look almost identical during the transient.

B. SCENARIO B: DRILLSTRING WITH A HORIZONTAL SECTION

We now consider a more realistic case with the presence of Coulomb friction terms. Compared to the previous scenario, the lowest part of the drilling device (collar and BHA) is now almost horizontal (MD= 2200 m now). In this scenario, the stationary drillstring is initially kept in place by the Coulomb friction until enough torque is built up to overcome it. Then, pipe rotation is initiated, and the Coulomb friction is reduced as it changes from static to dynamic. Negative torque is seen a the top drive to decelerate the motor inertia, but is not transferred to the attached pipe. We consider the switching mode procedure described in Section III-C to facilitate the estimation/cancellation of the disturbance. The torque is increased to break the static friction before starting the control procedure. The reference trajectory (66) remains unchanged. Then, the disturbance term is seen as a constant that can be directly compensated using the procedure developed in Section VII. We consider state-feedback controllers here since the objective is to compare the performance of the different controllers in an ideal case. The performance of the different algorithms are shown in Figure 7 (temporal evolution of the downhole angular velocity and of the motor torque). Here, one can easily notice the importance of the feedforward component and the disturbance cancellation term to reduce the oscillations induced by the Coulomb friction terms. Indeed, in the absence of the feedforward term, the ZTorque controller induces high oscillation for the angular velocity in steady-state (which implies a considerable performance degradation). Although oscillations are still present with the feedforward term, their amplitude has been considerably reduced. Once again, the recursive controller presents the

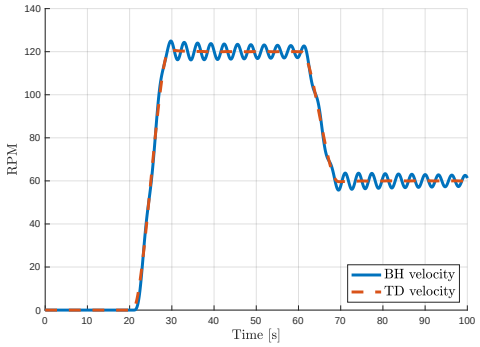

(a) ZTorque: angular velocities

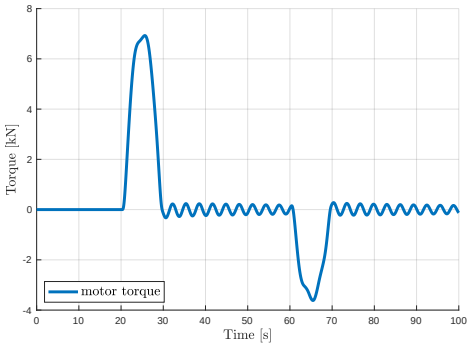

(b) ZTorque: motor torque

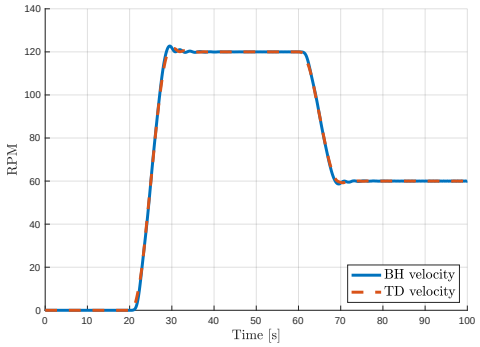

(c) ZTorque + feedforward: angular velocities

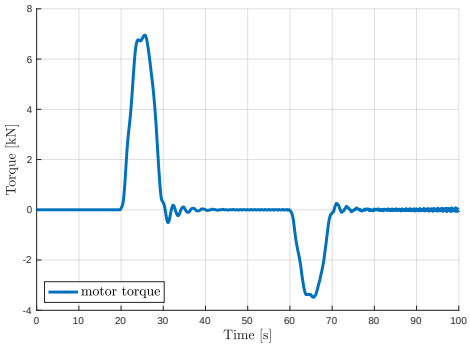

(d) ZTorque + feedforward: motor torque

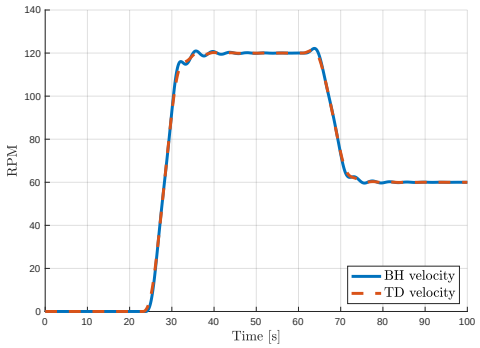

(e) MID algorithm: angular velocities

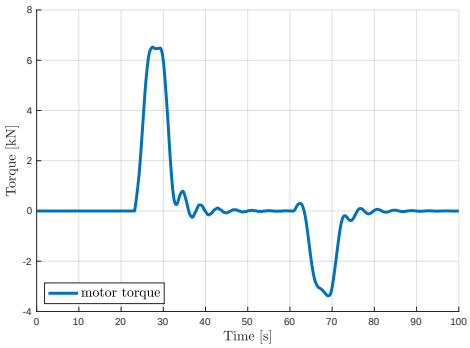

(f) MID algorithm: motor torque

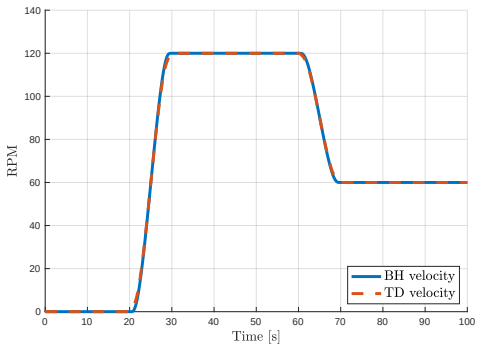

(g) Recursive algorithm: angular velocities

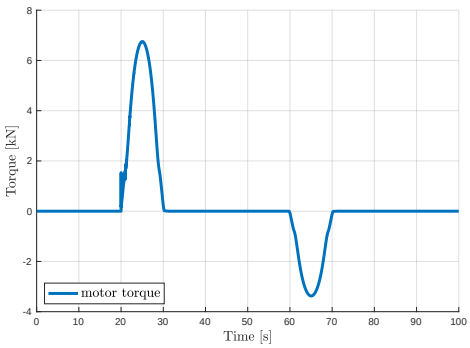

(h) Recursive algorithm: motor torque

FIGURE 6: Comparison of response to velocity set-point changes in terms of downhole angular velocity and motor torque τ_m for: (a,b) ZTorque feedback controller, (c,d) ZTorque feedback controller with the proposed differential flatness trajectory planning feed-forward component, (e,f) the MID feedback law, (g,h) the recursive algorithm (50). Set-point changes uses the mollifier (31) with a t_{sr} = 10 s switching duration. All the simulations are performed in the absence of Coulomb friction terms and under a 30 kN torque saturation constraint (MD=1500m).

best behavior (no overshoot and oscillations and fast convergence). However there is now an undesirable initial transient with a substantial control effort to compensate for the disturbance. Note that once, the disturbance term is cancelled, the change of set point is smooth. The MID procedure now presents a better behavior (at least in steady-state, once the disturbance-term is cancelled) compared to the feedforward procedure (almost no oscillation and an admissible control effort). Moreover, compared to the recursive procedure, this procedure is numerically less complex (most of the computations can be done offline). This test case emphasizes the potential advantages of the proposed alternative approaches compared to industry-standards controllers in the presence of important friction effects.

C. SCENARIO C: S-SHAPE WELLBORE

In this last scenario, we consider the complete S-shape wellbore pictured in Figure 5 (MD=3200m), which means that the Coulomb side-forces now act on a subsequent part of the drilling device. We still consider the switching mode procedure described in Section III-C to facilitate the estimation/cancellation of the disturbance. The reference trajectory (66) remains unchanged. We have pictured in Figure 8 the time-evolution of the downhole angular velocity and the motor torque. Due to the considerable impact of the Coulomb side-forces in this scenario, we have low-pass filtered the control input to reduce oscillations. We did not picture the performance of the standard ZTorque controller as it was failing to reach the reference without a reasonable amount of oscillations. Performance is considerably degraded due to the difficulties in compensating the friction terms and the angular velocity of the drillstring experiences high oscillation in steady-state. This could be expected as state-of-the-art controllers do not usually handle well such a configuration [28]. However, the oscillations remain in an acceptable range which underlines the promising potentials of the approaches we propose in the paper. Moreover, there is now a considerable delay between the reference signal and the real state. This is because compensation of the disturbance term is now more demanding. However, it can be easily overcome by anticipating this delay. From the plots, we can notice that the feedforward controller presents significant oscillations compared to the two other ones. The MID procedure presents a significant overshoot. However, it offers a satisfying behavior in steady state.

D. COMPARISON BETWEEN THE DIFFERENT ALGORITHMS

To simplify a comparison of the three controllers, we present a graphical comparison of the performance of the different control methods we have presented in this paper to suppress drilling vibrations. The radar chart given in Figure 9 allows examining, in a simple manner, the results obtained with the different control approaches with respect to some industrial implementation criteria, which include ease of implementation (both computationally and difficulty of integration in industrial motor controllers), performance and robustness to noise, latency and delay.. The results have been summarized in Table 2 presented in Section II-F. Thus, we only give a global comparison in this section. The basic ZTorque controller is the simplest one, but it does not mitigate stick-slip oscillations in the presence of significant friction. Combining it with a feedforward term and a disturbance compensation procedure allows a substantial reduction of the oscillations. The MID procedure is slightly more complex but can better handle the oscillations induced by the friction terms in complex geometries. Nevertheless, it creates a significant overshoot and requires time-derivative of the measurement (which implies the development of filtering strategies). Finally, the recursive algorithm is the most efficient one as it fully encompasses the dynamics of the system. However, it requires high instantaneous torque and is complex to implement (high computational effort and design of predictors). To avoid noise sensitivity, it is important to combine it with a low-pass filter. The good design of such a filter is out of the scope of this paper [59]. Note that although we did not consider the robustness properties of the different controllers, we believe that they are robust to small uncertainties in the parameters. This should be shown adjusting the time-delay approach proposed in [33] or in [27]. Moreover, the filtering strategy would guarantee the robustness with respect to delays [59].

IX. IMPLEMENTATION REQUIREMENTS

Modern drilling rigs found in the field have AC motors in top drives which are controlled via variable frequency drives (VFD). A typical variable frequency drive has a built-in proportional-integral (PI) controller with a 1-10 ms control loop. The default implementation for an off-the-shelf top drive is stiff speed control, where the P and I gains are high (typical values of $k_p = 10000, k_i = 3000$). VFDs are typically controlled via fiber optic, ethernet or analog connections to the central rig network, and are capable of handling small amounts (10 to 20 instructions) of embedded code. Systems such as SoftTorque and ZTorque are typically implemented as either embedded programming in the VFD or via bolt on cards connected via ethernet or analog input/outputs. These bolt on implementations suffer from increased signal delay (between 5 and 50 ms) which can reduce controller performance. Rig networks typically operate at 10 to 100 ms and supervisory control systems typically operate at 200 to 1000 ms. The complexity of the control solution dictates at which implementation level the controller may operate, which in turn, dictates controller performance. A thorough review of latency and delay, and the effects on drilling control, was presented by Cayeux et al. [66].

X. CONCLUSION

In this paper, we have presented three control algorithms that achieve angular velocity regulation for directional drilling operations. These strategies are designed to avoid torsional stick-slip oscillations at the start-up of a drilling operation,

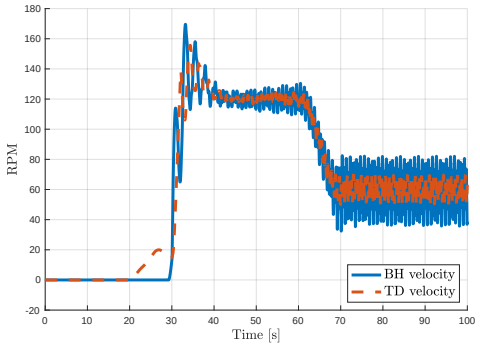

(a) ZTorque: angular velocities

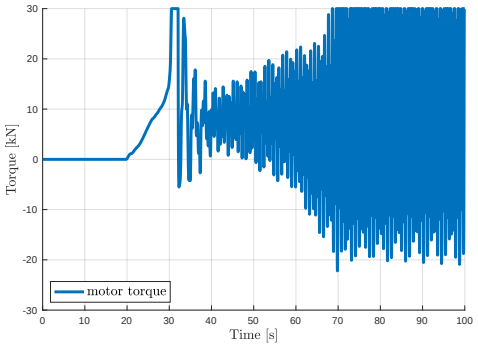

(b) ZTorque: motor torque

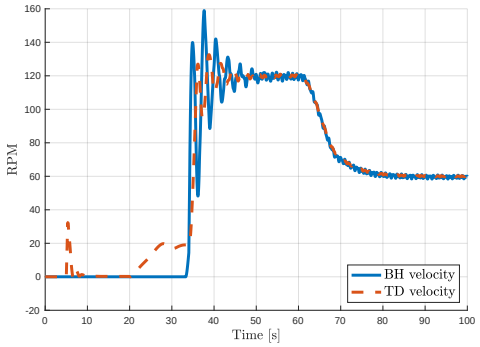

(c) ZTorque + feedforward: angular velocities

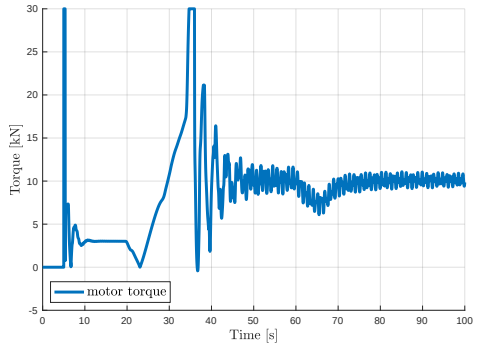

(d) ZTorque + feedforward: motor torque

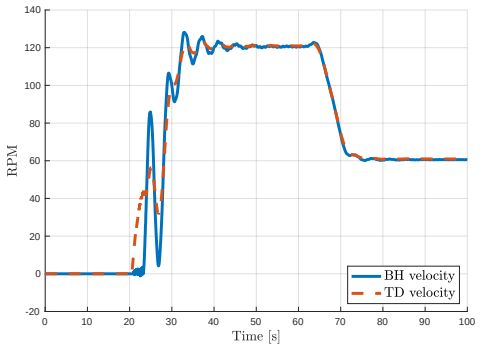

(e) MID algorithm: angular velocities

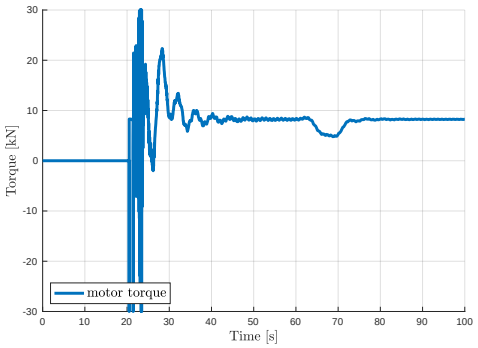

(f) MID algorithm: motor torque

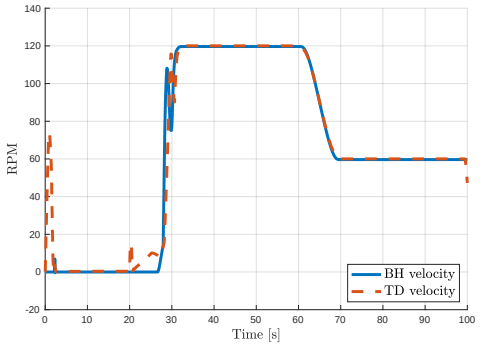

(g) Recursive algorithm: angular velocities

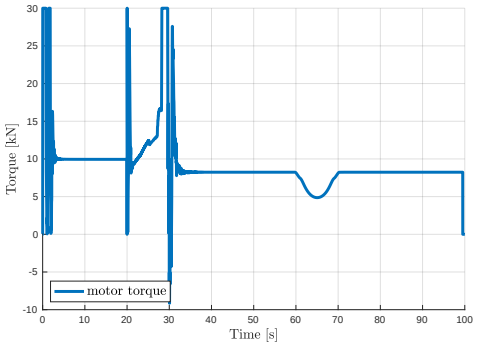

(h) Recursive algorithm: motor torque

FIGURE 7: Comparison of response to velocity set-point changes in terms of downhole angular velocity and motor torque τ_m for: (a,b) ZTorque feedback controller, (c,d) ZTorque feedback controller with the proposed differential flatness trajectory planning feed-forward component, (e,f) the MID feedback law, (g,h) the recursive algorithm (50). Set-point changes uses the mollifier (31) with a t_{sr} = 10 s switching duration. All the simulations are performed for a well with a horizontal collar part and under a 30 kN torque saturation constraint (MD=1700m).

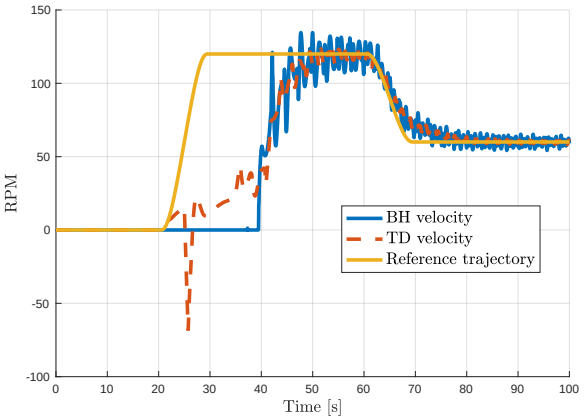

(a) ZTorque + feedforward: angular velocities

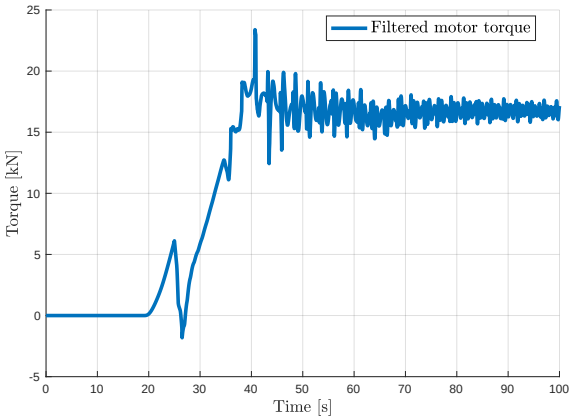

(b) ZTorque + feedforward: motor torque

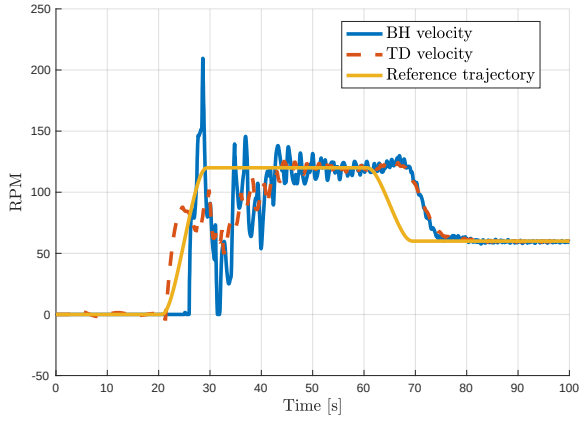

(c) MID algorithm: angular velocities

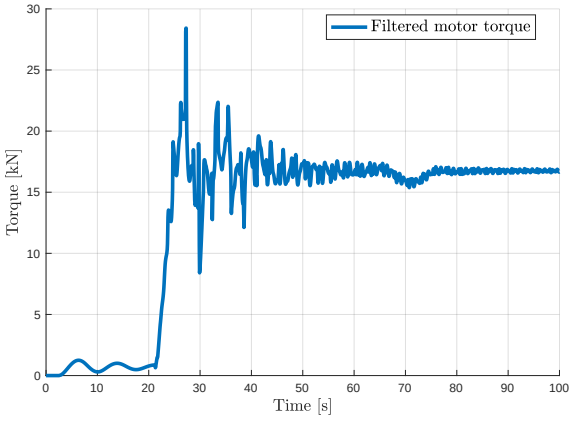

(d) MID algorithm: motor torque

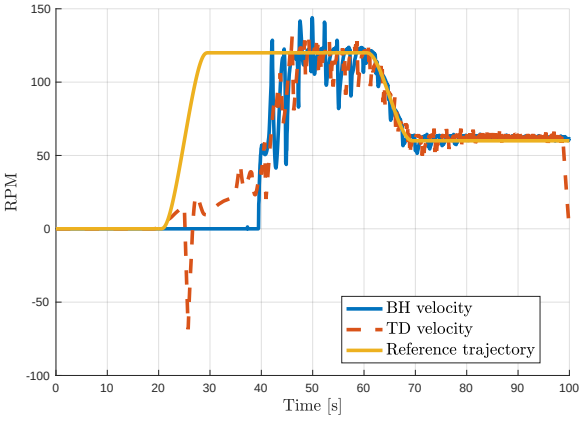

(e) Recursive algorithm: angular velocities

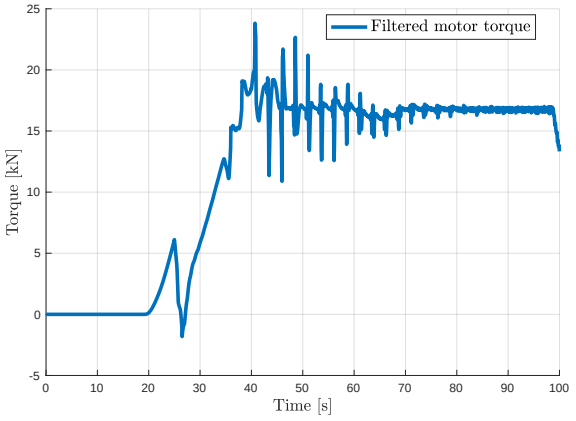

(f) Recursive algorithm: motor torque

FIGURE 8: Comparison of response to velocity set-point changes in terms of downhole angular velocity and motor torque τ_m for: (a,b) ZTorque feedback controller with the proposed differential flatness trajectory planning feed-forward component, (c,d) the MID feedback law, (e,f) the recursive algorithm (50). Set-point changes uses the mollifier (31) with a t_{sr} = 10 s switching duration. All the simulations are performed for a S-shape well and under a 30 kN torque saturation constraint (MD=2000m). The control input is low-pass filtered

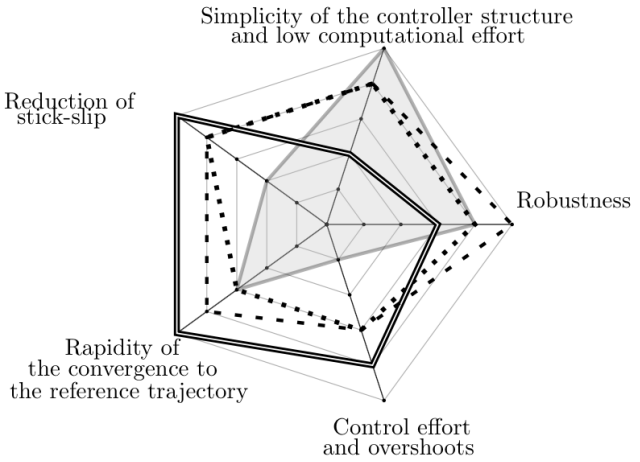

FIGURE 9: Radar diagram illustrating the performance of the proposed controllers on various assessment aspects related to the drilling torsional dynamics. There are four polygons with different contours; each one of them corresponds to a different control strategy: lightgray for the ZTorque controller, loosely dotted for ZTorque feedback controller with the proposed differential flatness trajectory planning feedforward component, double line for the recursive algorithm, and loosely dashed for the MID procedure.

e.g., after a connection. The first strategy corresponds to the industry standard ZTorque controller, to which is added a feedforward component and disturbance compensation terms. It corresponds to an extension of [28] for a multi-sectional drilling device. Although simple to implement and with a low computational effort, such a procedure cannot cancel all the oscillations induced by the stick-slip phenomenon. The second procedure corresponds to a pole placement for the downhole state. It presents satisfying performance and is robust to parameter uncertainties. Moreover most of the computations can be done offline, which results in a simple control algorithm. However, it requires a derivative term (that can be sensitive to noise) but it does not mitigate stick-slip oscillations in the presence of significant friction. Finally, the last procedure relies on a recursive interconnected dynamics framework. It presents excellent performance at the cost of a high instantaneous control effort. However, its complexity may imply a substantial computational cost (as it requires estimating the different states of the PDEs). These three procedures have been validated on a high-fidelity simulator that has been shown to reproduce, in open-loop simulations, the dynamics of a drilling system during start-up. Their performance have been compared on several test-cases (bit off-bottom). Future improvements include reducing the numerical complexity of the different control strategies. A possible path to follow would consist in emulating the PDE describing the motion of the drilling device using deep learning algorithms. This would considerably reduce the estimation procedure while enabling satisfying estimates of the friction parameters. Such an estimation procedure could then be tested against field data to obtain a complete analysis of the inherent computational effort. The use of an event-triggered output-feedback law (as presented in [67]) could also avoid useless actuator solicitations. Another topic of future investigations will consists in adjusting the proposed algorithms in the case of a coupled axial-torsional dynamics with bit-rock interaction.

ACKNOWLEDGMENTS

The authors thank the Associate Editor and the reviewers for their comments that considerably improved the quality of the paper. This work was in part supported by the University of Calgary's Canada First Research Excellence Fund Program, the Global Research Initiative in Sustainable Low Carbon Unconventional Resources.

JEAN AURIOL (M'2021) received his Master degree in civil engineering in 2015 (major: applied maths) in MINES ParisTech, part of PSL Research University and in 2018 his Ph.D. degree in control theory and applied mathematics from the same university (Centre Automatique et Systèmes). His Ph.D. thesis, titled Robust design of backstepping controllers for systems of linear hyperbolic PDEs, has been nominated for the best thesis award given by the GDR MACS and the Section Automatique du Club EEA in France. From 2018 to 2019, he was a Postdoctoral Researcher at the Department of Petroleum Engineering, University of Calgary, AB, Canada, where he was working on the implementation of backstepping control laws for the attenuation of mechanical vibrations in drilling systems. From December 2019, he is a Researcher (Chargé de Recherches) at CNRS, Université Paris-Saclay, Centrale Supelec, Laboratoire des Signaux et Systèmes (L2S), Gif-sur-Yvette, France. His research interests include robust control of hyperbolic systems, neutral systems, networks and interconnected systems.

ISLAM BOUSSAADA (M'2021) received his M.Sc. degree in Mathematics from University of Carthage as well as an M.Sc. degree in Pure Mathematics from University Paris 7 in 2004. In December 2008, he received his Ph.D. degree in Mathematics from Normandy University. In 2016 he obtained the French habilitation (HDR) in Physics from University Paris Saclay. In 2010, IB was appointed for one year as a post-doctoral fellow in the control of time-delay systems at L2S, Université Paris Saclay, CentraleSupelec-CNRS. From September 2011 until September 2017, he has been an associate professor at IPSA and an associate researcher at MODESTY Team of L2S. Since October 2017, IB is appointed as an associate researcher at DISCO Team Inria Saclay and full professor at IPSA. His research interest belongs to the field of the qualitative theory of dynamical systems and its application in control. It covers the analysis of the delay effect on dynamics, stability and stabilization of delay system and hyperbolic partial differential equations, oscillations and periodic solutions of functional differential equations, control of vibrations, analysis and control of biochemical reactions. He authored or co-authored 2 monographs and more than 90 papers in journals, book chapters and international conferences' proceedings.

ROMAN J. SHOR is an associate professor in the Department of Chemical and Petroleum Engineering at the University of Calgary, leads the Drilling Research Lab and co-leads the Geothermal Energy Lab. His current research focuses on real-time and reduced order modelling of the drilling system, modelling for control, control system design for both supervisory and machine control and applications of machine learning and artificial intelligence to drilling engineering problems. Dr. Shor received his doctorate in Petroleum Engineering from the University of Texas at Austin and his Master's and Bachelor's in Computer Science from the University of Pennsylvania. For further information, please visit https://schulich.ucalgary.ca/contacts/roman-shor

HUGUES MOUNIER received the Ph.D. degree in automatic control from Laboratoire des Signaux et Systèmes, Université Paris Sud, Orsay, France, in 1995. From 1998 to 2010, he was with Institut d'Electronique Fondamentale, Université Paris Sud. He is currently a Professor with the Laboratoire des Signaux et Systèmes. His research interests include automotive and real-time control, neuro-science, delay systems and systems modeled by partial differential equations.

SILVIU-IULIAN NICULESCU received the B.S. degree from the Polytechnical Institute of Bucharest, Romania, the M.Sc., and Ph.D. degrees from the Institut National Polytechnique de Grenoble, France, and the French Habilitation (HDR) from Université de Technologie de Compiègne, all in Automatic Control, in 1992, 1993, 1996, and 2003, respectively. He is currently Research Director at CNRS (French National Center for Scientific Research), L2S (Laboratory of Signals and Systems), a joint research unit of CNRS with CentraleSupelec and Université Paris-Saclay located at Gif-sur-Yvette. Dr. Niculescu is a member of the Inria team "DISCO" and he was the head of L2S for a decade (2010-2019). He is author/coauthor of 11 books and of more than 550 scientific papers. His research interests include delay systems, robust control, operator theory, and numerical methods in optimization, and their applications to the design of engineering systems. Since 2017, he is the Chair of the IFAC TC "Linear Control Systems" and he served as Associate Editor for several journals in Control area, including the IEEE Transactions on Automatic Control (2003-2005). IEEE Fellow since 2018, Doctor Honoris Causa of University of Craiova (Romania) since 2016, Founding Editor and Editor-in-Chief of the Springer Nature Series "Advances in delays and dynamics" since its creation in 2012, Dr. Niculescu was awarded the CNRS Silver and Bronze Medals for scientific research and the Ph.D. Thesis Award from Grenoble INP (France) in 2011, 2001 and 1996, respectively. For further information, please visit https://cv.archives-ouvertes.fr/silviu-iulian-niculescu

REFERENCES

[1] M. Kapitaniak, V. V. Hamaneh, J. P. Chávez, K. Nandakumar, and M. Wiercigroch. Unveiling complexity of drill–string vibrations: Experiments and modelling. International Journal of Mechanical Sciences, 101:324–337, 2015.

[2] P.D. Spanos, A.M. Chevallier, N. P. Politis, and M. L. Payne. Oil and gas well drilling: a vibrations perspective. The Shock and Vibration Digest, 35(2):85–103, 2003.

[3] V. A. Dunayevsky and F. Abbassian. Application of Stability Approach to Bit Dynamics. SPE Drilling & Completion, 13(2):22–25, jun 1998.

[4] J. D. Jansen. Nonlinear dynamics of oilwell drillstrings. PhD thesis, Delft University of Technology, 1993.

[5] B. Saldivar, S. Mondié, J.-J. Loiseau, and V. Rasvan. Stick-slip oscillations in oillwell drilstrings: Distributed parameter and neutral type retarded model approaches. IFAC Proceedings Volumes (IFAC-PapersOnline), 18(PART 1):284–289, 2011.

[6] K. Nandakumar and M. Wiercigroch. Stability analysis of a state dependent delayed, coupled two DOF model of drill-string vibration. Journal of Sound and Vibration, 332(10):2575–2592, may 2013.

[7] U. J. Aarsnes and R. J. Shor. Torsional vibrations with bit off bottom: Modeling, characterization and field data validation. Journal of Petroleum Science and Engineering, 163:712–721, apr 2018.

[8] J. S. Mason, M. Sprawls, et al. Addressing bha whirl-the culprit in mobile bay. In SPE/IADC Drilling Conference, number 04, pages 231–236. Society of Petroleum Engineers, 1996.

[9] P. C. Kriesels, W . J. G. Keultjes, P. Dumont, I. Huneidi, O.O. Owoeye, R. A. Hartmann, et al. Cost savings through an integrated approach to drillstring vibration control. In SPE/IADC Middle East Drilling Technology Conference. Society of Petroleum Engineers, 1999.

[10] J. M. Kamel and A. S. Yigit. Modeling and analysis of stick-slip and bit bounce in oil well drillstrings equipped with drag bits. Journal of Sound and Vibration, 333(25):6885–6899, 2014.

[11] B. Saldivar, S. Mondié, S.-I. Niculescu, H. Mounier, and I. Boussaada. A control oriented guided tour in oilwell drilling vibration modeling. Annual Reviews in Control, 42:100–113, 2016.

[12] J. Bailey and I. Finnie. An analytical study of drill-string vibration. Journal of Manufacturing Science and Engineering, 82, 1960.

[13] J. Rudat, D. Dashevskiy, and L. Pohle. Model-based stability analysis of torsional drillstring oscillations. In 2011 IEEE International Conference on Control Applications (CCA), pages 501–508. IEEE, 2011.

[14] R I Leine, D H van Campen, and W J G Keultjes. Stick-slip Whirl Interaction in Drillstring Dynamics. Journal of Vibration and Acoustics, 124(2):209, 2002.

[15] J. F. Brett, A. D. Beckett, C. A. Holt, and D. L. Smith. Uses and Limitations of Drillstring Tension and Torque Models for Monitoring Hole Conditions. SPE Drilling Engineering, 4(03):223–229, sep 1989.

[16] G. W. Halsey, A. Kyllingstad, T. V. Aarrestad, and D. Lysne. Drillstring Vibrations: Comparison Between Theory and Experiments on a Full-Scale Research Drilling Rig. In SPE/IADC Drilling Conference, number IADC/SPE 14760, pages 311–321. Society of Petroleum Engineers, apr 1986.

[17] D. Zhao, S. Hovda, and S. Sangesland. Abnormal Down Hole Pressure Variation by Axial Stick-Slip of Drillstring. Journal of Petroleum Science and Engineering, 145:194–204, 2016.

[18] E. Detournay and P. Defourny. A phenomenological model for the drilling action of drag bits. International Journal of Rock Mechanics and Mining Sciences & Geomechanics Abstracts, 29(1):13–23, 1992.

[19] T. Richard, C. Germay, and E. Detournay. Self-excited stick-slip oscillations of drill bits. Comptes Rendus Mécanique, 332(8):619–626, aug 2004.

[20] R.I. Leine. Literature survey on torsional drillstring vibrations. Division of Computational and Experimental Mechanics, Department of Mechanical Engineering Eindhoven University of Technology. The Netherlands, 1997.

[21] Å. Kyllingstad and P. J. Nessjøen. A New Stick-Slip Prevention System. In Proceedings of SPE/IADC Drilling Conference and Exhibition, number March, pages 17–19, 2009.

[22] S. Dwars. Recent Advances in Soft Torque Rotary Systems. In Proceedings of 2015 SPE/IADC Drilling Conference, number March, pages 17–19, 2015.

[23] E. M Navarro-López and D. Cortés. Sliding-mode control of a multi-dof oilwell drillstring with stick-slip oscillations. In 2007 American control conference, pages 3837–3842. IEEE, 2007.

[24] B. Besselink, T. Vromen, N. Kremers, and N. Van De Wouw. Analysis and control of stick-slip oscillations in drilling systems. IEEE transactions on control systems technology, 24(5):1582–1593, 2015.

[25] T. Vromen, N. Van De Wouw, A. Doris, P. Astrid, and H. Nijmeijer. Nonlinear output-feedback control of torsional vibrations in drilling systems. International Journal of Robust and Nonlinear Control, 27(17):3659–3684, 2017.

[26] D. J. Runia, S. Dwars, and I. P. J. M. Stulemeijer. A brief history of the Shell "Soft Torque Rotary System" and some recent case studies. In SPE/IADC Drilling Conference, pages 69–76. Society of Petroleum Engineers, mar 2013.

[27] J. Auriol. Robust design of backstepping controllers for systems of linear hyperbolic PDEs. PhD thesis, PSL Research University, 2018.

[28] U. J. F. Aarsnes, F. Di Meglio, and R. J. Shor. Avoiding stick slip vibrations in drilling through startup trajectory design. Journal of Process Control, 70:24–35, 2018.

[29] I. Boussaada, H. U. Unal, and S.-I. Niculescu. Multiplicity and stable varieties of time-delay systems: A missing link. In 22rd International Symposium on Mathematical Theory of Networks and Systems, pages 55–60, 2016.

[30] I. Boussaada, S. Tliba, S.-I. Niculescu, H. U. Ünal, and T. Vyhlídal. Further remarks on the effect of multiple spectral values on the dynamics of time-delay systems. application to the control of a mechanical system. Linear Algebra and its Applications, 542:589–604, 2018.

[31] D. Ma, I. Boussaada, C. Bonnet, S-I. Niculescu, and J. Chen. Multiplicity-Induced-Dominancy extended to neutral delay equations: Towards a systematic PID tuning based on Rightmost root assignment. In ACC 2020 - American Control Conference, Denver, United States, July 2020.

[32] A. Benarab, I. Boussaada, G. Trabelsi, K.and Mazanti, and C. Bonnet. The MID property for a second-order neutral time-delay differential equation. In 2020 24th International Conference on System Theory, Control and Computing, pages 202–207, 2020.

[33] J. Auriol, I. Boussaada, H. Mounier, and S. I. Niculescu. Torsional-vibrations damping in drilling systems: Multiplicity-induced-dominancy based design. In 24th International Symposium on Mathematical Theory of Networks and Systems, pages 428–433. IFAC, 2021.

[34] D. Ma, I. Boussaada, J. Chen, C. Bonnet, S-I. Niculescu, and J. Chen. PID control design for first-order delay systems via mid pole placement: Performance vs. robustness. Automatica, 286:84–118, 2022.

[35] T. Vyhlidal, W. Michiels, and P. Zitek. Quasi-direct pole placement for time delay systems applied to a heat transfer set-up. IFAC Proceedings Volumes, 42(14):325–330, 2009. 8th IFAC Workshop on Time-Delay Systems.

[36] Y.M. Ram, J.E. Mottershead, and M.G. Tehrani. Partial pole placement with time delay in structures using the receptance and the system matrices. Linear Algebra and its Applications, 434(7):1689–1696, 2011. Special Issue: NIU.

[37] J. Redaud, J. Auriol, and S.-I. Niculescu. Output-feedback control of an underactuated network of interconnected hyperbolic PDE-ODE systems. Sytems and Control Letters, 2021.

[38] J. Auriol. Output feedback stabilization of an underactuated cascade network of interconnected linear pde systems using a backstepping approach. Automatica, 117:108964, 2020.

[39] J. Auriol, N. Kazemi, and S-I Niculescu. Sensing and computational frameworks for improving drill-string dynamics estimation. Mechanical Systems and Signal Processing, 160:107836, 2021.

[40] U. J. F. Aarsnes, J. Auriol, F. Di Meglio, and R. J. Shor. Estimating friction factors while drilling. Journal of Petroleum Science and Engineering, 179:80–91, 2019.

[41] C. Germay, V. Denoël, and E. Detournay. Multiple mode analysis of the self-excited vibrations of rotary drilling systems. Journal of Sound and Vibration, 325(1-2):362–381, aug 2009.

[42] M C Sheppard, C Wick, and T Burgess. Designing Well Paths To Reduce Drag and Torque. SPE Drilling Engineering, 2(04):344–350, dec 1987.

[43] U. J. F. Aarsnes and O. M. Aamo. Linear stability analysis of self-excited vibrations in drilling using an infinite dimensional model. Journal of Sound and Vibration, 360:239–259, jan 2016.

[44] U. J. F Aarsnes, O. M. Aamo, and M. Krstic. Extremum seeking for real-time optimal drilling control. In 2019 American Control Conference (ACC), pages 5222–5227. IEEE, 2019.

[45] F. Di Meglio and Ulf J. F. Aarsnes. A distributed parameter systems view of control problems in drilling. IFAC-PapersOnLine, 48(6):272–278, 2015.

[46] T. Richard, C. Germay, and E. Detournay. A simplified model to explore the root cause of stick–slip vibrations in drilling systems with drag bits. Journal of Sound and Vibration, 305(3):432–456, aug 2007.

[47] R. J. LeVeque. Finite volume methods for hyperbolic problems. Cambridge university press, 2002.

[48] J. Deutscher and J. Gabriel. A backstepping approach to output regulation for coupled linear wave–ode systems. Automatica, 123:109338, 2021.

[49] K. J. Aström and R. M. Murray. Feedback systems: an introduction for scientists and engineers. Princeton university press, 2010.

[50] T. Knüppel, F. Woittennek, I. Boussaada, H. Mounier, and S.-I. Niculescu. Flatness-based control for a non-linear spatially distributed model of a drilling system. In Low-Complexity Controllers for Time-Delay Systems, pages 205–218. Springer, 2014.

[51] A. Kyllingstad. A Comparison of Stick-Slip Mitigation Tools. In SPE/IADC Drilling Conference and Exhibition, number March, pages 14–16. Society of Petroleum Engineers, mar 2017.

[52] G. W. Halsey, A. Kyllingstad, and A. Kylling. Torque Feedback Used to Cure Slip-Stick Motion. In SPE Annual Technical Conference and Exhibition, pages 277–282. Society of Petroleum Engineers, apr 1988.

[53] U. J. F. Aarsnes, F. di Meglio, and R. Shor. Benchmarking of industrial stick-slip mitigation controllers. IFAC-PapersOnLine, 51(8):233–238, 2018.

[54] I. Boussaada, H. Mounier, and S.I. Niculescu. Low complexity controllers for vibrations damping in drilling systems. In 2019 American Control Conference (ACC), pages 5228–5233. IEEE, 2019.

[55] V. Rasvan. A method for distributed parameter control systems and electrical networks analysis. Revue Roumaine des Sciences Techniques, 20, 1975.

[56] S. Fueyo, G. Mazanti, I. Boussaada, Y. Chitour, and S.I. Niculescu. Insights into the multiplicity-induced-dominancy for scalar delay-differential equations with two delays. 2021.

[57] J. Auriol, N. Kazemi, R. J. Shor, K. A. Innanen, and I. D. Gates. A sensing and computational framework for estimating the seismic velocities of rocks interacting with the drill bit. IEEE Transactions on Geoscience and Remote Sensing, 58(5):3178–3189, 2019.

[58] N. Gehring. A systematic design of backstepping-based state feedback controllers for ode-pde-ode systems. IFAC-PapersOnLine, 54(9):410–415, 2021.

[59] D. Bou Saba, F. Bribiesca-Argomedo, M. Di Loreto, and D. Eberard. Strictly proper control design for the stabilization of $2\times$ 2 linear hyperbolic ode-pde-ode systems. In 2019 IEEE 58th Conference on Decision and Control (CDC), pages 4996–5001. IEEE, 2019.

[60] J. Auriol, J. Deutscher, G. Mazanti, and G. Valmorbida. Advances in Distributed Parameter Systems. Springer, 2021 (to appear).

[61] F. di Meglio, P.O. Lamare, and U. J. Aarsnes. Robust output feedback stabilization of an ODE–PDE–ODE interconnection. Automatica, 119, 2020.

[62] I. Karafyllis and M. Krstic. Predictor feedback for delay systems: Implementations and approximations. Springer, 2017.

[63] N. Bekiaris-Liberis. Simultaneous compensation of input and state delays for nonlinear systems. Systems and Control Letters, 73:96–102, 2014.

[64] D. Bresch-Pietri and F. Di Meglio. Prediction-based control of linear input-delay system subject to state-dependent state delay-application to suppression of mechanical vibrations in drilling. Proc. of the 2nd IFAC Workshop on Control of Systems Governed by Partial Differential Equations, 49(8):111–117, 2016.

[65] R. Courant, K. Friedrichs, and H. Lewy. On the partial difference equations of mathematical physics. IBM journal of Research and Development, 11(2):215–234, 1967.

[66] E. Cayeux. On the Importance of Boundary Conditions for Real-Time Transient Drill-String Mechanical Estimations. In IADC/SPE Drilling Conference and Exhibition. Society of Petroleum Engineers, mar 2018.

[67] N. Espitia. Observer-based event-triggered boundary control of a linear $2\times$ 2 hyperbolic systems. Systems & Control Letters, 138:104668, 2020.